WEICHENG ZHANG
Growth and differentiation of N1E-115 neuroblastoma cells in High Aspect Rotating Vessel (HARV) under hypoxia, normoxia and hyperoxia.
(Under Direction of WILLIAM SSEMPA KISAALITA)

The general purpose of this study was to confirm or rule out the possibility that microgravity and hypoxia were factors in the previously observed culture color change, from yellow to black/brown in differentiation of N1E-115 neuroblastoma cells cultured under simulated microgravity. In this study, N1E-115 cells were cultured and differentiated under microgravity on cytodex 3 beads in HARV bioreactor. Control cultures were differentiated under normal gravity in petri and tissue culture dishes. The culture vessels were operated in a CO_2 incubator at different incubator oxygen levels of hypoxia (10%), normoxia (18%) and hyperoxia (26%). It was not possible to replicate color development by differentiating neuroblastoma cells under simulated microgravity suggesting that the phenomena previously observed in our laboratory and by other investigations was not solely dependent on microgravity, if at all. Metabolic differences (O_2 consumption pattern) observed between cells differentiated under normal and microgravity were attributed more to O_2 mass transport limitation into the HARV. Also, hopoxia was not proven to be a factor in transdifferentiation of N1E-115 neuroblastoma cells to melanocyte-like cells.

INDEX WORDS: N1E-115 Neuroblastoma cell, cell differentiation, microgravity, High Aspect Rotation Vessel (HRAV), hypoxia, normoxia, hyperoxia, pigment cell, tyrosinase.

GROWTH AND DIFFERENTIATION OF N1E-115 NEUROBLASTOMA CELLS IN HIGH ASPECT ROTATING VESSEL (HARV) UNDER HYPOXIA, NORMOXIA AND HYPEROXIA.

by

WEICHENG ZHANG

BENG, Beijing Institute of Light Industry, China, 1988

MENG, Beijing Institute of Light Industry, China, 1993

A Thesis Submitted to the Graduate Faculty

of The University of Georgia in Partial Fulfillment

of the Requirements for the Degree

MASTER OF SCIENCE

ATHENS, GEORGIA

2001

GROWTH AND DIFFERENTIATION OF N1E-115 NEUROBLASTOMA CELLS IN HIGH ASPECT ROTATING VESSEL (HARV) UNDER HYPOXIA, NORMOXIA AND HYPEROXIA.

by

WEICHENG ZHANG

Approved:

Major Professor: Dr. William S. Kisaalita

Committee: Dr. Charles H. Keith
Dr. Timothy L. Foutz

Electronic Version Approved:

Gordhan L. Patel
Dean of the Graduate School
The University of Georgia
December 2001

To my family for their love and support

ACKNOWLEDGEMENTS

Special thanks to my major professor Dr. William S. Kisaalita for his open minded guidance, direction and patience during the entire course of my Masters study. I also thank Drs. Charles Keith and Tim Foutz for serving on my advisory committee and providing me with guidance and new ideas.

I am deeply grateful to Dianne Stroman and Melissa Bishop for their technical support, and to Sarah Lee in Dr. Eiteman's lab for glucose analysis.

I would also like to thank my friends and colleagues in the Cellular Engineering Laboratory, Mike Yoder, Raj Rao, Adam Singer and Chen Mao for their companionship and for sharing their research experience. I would also like to thank all the people in the department for their kind help which was available whenever I needed it.

Last, I thank my parents and brothers on the other side of the globe for their constant encouragement and support throughout my life; to them I dedicate my further studies.

TABLE OF CONTENTS

CHAPTER 1

INTRODUCTION

The N1E-115 cell line was derived from a spontaneously arising murine neuroblastoma, C1300, and has been widely used to study in vitro differentiation (Amano et al, 1972). When differentiated in vitro, N1E-115 cells exhibit neurite outgrowth and develop an excitable membrane. In vitro differentiation is controlled by many factors including the growth substrate, cell-cell recognition molecules and the presence of growth factors in the extracellular medium (Cosgrove et al, 1991). Maintenance of N1E-115 cells in extremely low serum conditions is an effective trigger for in vitro differentiation.

We have previously used flow cytometry and a voltage sensitive oxonol dye to demonstrate that N1E-115 cells differentiate to nerve-like cells in conventional culture dishes, characterized by a rise in resting membrane potential between 7 and 12 days (Kisaalita et al, 1997). Also, differentiating N1E-115 cells exposed to developmental toxicants (retinoids and acetylsalicyclic acid) exhibited the greatest vulnerability in terms of cell death during a period of 8 to 10 days after incubation in differentiating medium. Taken together, these results seem to suggest that the period from 7 to 12 days characterized very important physiological changes.

In preliminary experiments conducted by Dr. Marian Lewis at the Bioreactor Laboratory, Johnson Research Center, Huntsville, Alabama, N1E-115 neuroblastoma cells were observed to change color when differentiated under simulated microgravity

after 8 to 10 days of exposure to differentiating medium. These observations were replicated in our laboratory. N1E-115 cells differentiated under simulated microgravity exhibited a color change from yellow to brown/black during approximately the same period of 8 to 10 days. These qualitative observations seem to suggest the possibility of transdifferentiation of N1E-115 cells to pigmented cells in response to simulated microgravity. A similar phenomenon has been observed in the laboratory at the Department of Medicine, the University of Wisconsin Medical School with PC12 and other neuroblastoma cells. The color change was attributed to hypoxia (insufficient oxygen supply) and hypoglycemia (insufficient glucose feeding) or improper handling of the culture (Lelkes, personal communication, 2000).

Most of the literature on oxygen and neuroblastoma cells is concerned with using hypoxia and hyperbaric oxygen to treat neuroblastoma tumors (e.g., Cornelissen et al, 1997, Voute et al, 1995 and 1996, Goda et al, 1996). This suggests that changing dissolved oxygen may play a role in neuroblastoma cell differentiation, however, no reports were found specifically addressing the transdifferentiation of neuroblastoma cells.

The general purpose of this study was two-fold. First, to replicate the transdifferentiation of N1E-115 cells to pigmented cells with a goal of ruling out or confirming a role for simulated microgravity. Second, to investigate the effect of dissolved oxygen on N1E-115 cell differentiation in vitro under normal and simulated microgravity.

The current research focus in the Cellular Bioengineering Laboratory involves the development of cell based systems with applications in accelerated drug discovery. In light of this, the motivation to pursue N1E-115 transdifferentiation was based on two

potential benefits. First, understanding transdifferentiation of neuroblastoma into melanocyte-like cells may provide a convenient experimental system with which to determine the influence of microgravity on the development of neural crest and/or other nervous system cells in vitro and possibly in vivo. Second, the system has the potential to provide an in vitro melanoma model, which could lead to the determination of intracellular targets for drug discovery and elucidation of the transduction pathway.

REFERENCES

1. Amano, T.; Richelson, E.; Nirenberg, M. Neurotransmitter synthesis by neuroblastoma clones. *Proc. Natl. Acad. Sci.* USA. **1972**, 69, 258-263.
2. Cornelissen J.; A. B. P. VanKuilenburg; L. Elizinga. Hyperbaric oxygen enhances the effects of meta-iodobenzylguanidine (MIBG) on energy metabolism and lipid peroxidation in the human neuroblastoma cell line SK-N-BE (C). *Anticancer Research* **1997**, 17, 259-264.
3. Cosgrove C.; Peter Cobbett. Induction of temporally dissociated morphological and physiological differentiation of N1E-115 cells. *Brain Research Bulletin* **1991**, 27, 53-58.
4. Goda F; G. Bacic; J. A. O'Hara. The relationship between pO_2 and perfusion in to murine tumors after X-ray irradiation: a combined Gd-DTPA dynamic MRI and EPR oximetry study. *Cancer Research* **1996,** 56, 3344-3349.
5. Kisaalita, W. S.; J. M. Bowen. Development of resisting membrane potential in differentiating neuroblastoma cells (N1E-115) evaluated by flow cytometry. *Cytotechnology* **1997**, 24, 201-212.

6. Lelkes P. 2000. University of Wisconsin Medical School. Private communication.
7. Voute P. A.; A. J. Vanderkleij; J. Dekraker. Clinical experience with radiation enhancement by hyperbaric oxygen in children with recurrent neuroblastoma stage IV. *European Journal of Cancer* **1995**, 31A, 596-600.
8. Voute P. A.; M. M. C. TielvanBuul; A. J. Vanderkleij. Combined I-131-MIBG therapy and hyperbaric oxygen therapy in children with recurrent neuroblastoma. *Journal of Nuclear Medicine* **1996**, 37, 1282-1282.

CHAPTER 2

LITERATURE REVIEW

The study of biological processes under microgravity conditions is becoming an invaluable tool in directing and controlling biological processes. Analysis of biological processes in this environment spans a broad spectrum and includes fundamental issues such as cell growth, maintenance, and alterations in cell structure. Since microgravity affects prokaryotic and eukaryotic cell function at a cellular and molecular level, many of the physiological changes seen in humans, vertebrate and simple organisms in space flight may originate from adaptation of basic biological mechanisms to the microgravity environment.

Results from this area of study yield important new advances that can eventually lead to practical applications in biotechnology, such as efficiently producing biological tissue constructs using the reduced gravity environment.

GRAVITY AND MICROGRAVITY

Gravity is such an accepted part of our lives that we rarely think about it, even though it affects everything we do. Any time we drop or throw something and watch it fall to the ground, we see gravity in action. Although gravity is a universal force, there are times when it is not desirable to conduct scientific research under its full influence. In these cases, scientists perform their experiments in microgravity----a condition in which the effects of gravity are greatly reduced, sometimes described as “weightlessness.”

This description brings to mind images of astronauts and objects floating around inside an orbiting spacecraft, seemingly free of Earth's gravitational field, but these images are misleading. The pull of Earth's gravity actually extends far into space. To reach a point where Earth's gravity is reduced to one-million of that on Earth's surface, one would have to be 6.37 million kilometers away from Earth, it's almost 17 times farther away than the Moon. However, spacecraft usually orbit only 200-450 kilometers above Earth's surface.

Initial research into the effects of microgravity began in the early years of the space program on Apollo, Skylab and Apollo-Soyuz during 1960s and 1970s. After 1981, the space shuttle program initiated the development of microgravity research instruments that could be flown, modified, and flown again, enabling scientists to design experiments based on the results of previous investigations. The challenges facing microgravity research efforts today are to use ground-based facilities.

NASA-Johnson Space Center has several facilities that can provide a microgravity environment for scientific research (Figure 2.1, http://mgnews.msfc.nasa.gov/litho2/facility.html).

Figure 2.1 Illustrations of showing various ground and space based facilities that provide a microgravity environment for conducting scientific research

1) **Drop towers and tubes** are long shafts used for dropping experiments. While the experiments drop, they are in free fall or microgravity. The periods of microgravity provided by the 24 and 132 meter high drop towers and 105 meter high drop tube are 2.2, 5.2 and 4.6 seconds, respectively.
2) **Reduced-gravity aircrafts** are flown in parabolic arcs to achieve longer periods of microgravity. Usually 20-25 seconds.
3) **Sounding rockets** produce higher quality microgravity conditions for longer periods than airplanes or drop towers and tubes and usually experience several minutes of microgravity before the rocket re-enters the atmosphere.
4) **The Space shuttle** is a spacecraft that often carries special laboratories for conducting scientific research. It can stay in the orbit around the Earth up to 17 days.
5) **The Space station** is a spacecraft that can remain in Earth's orbit for as long as several decades.

CELLULAR GROWTH AND/OR DIFFERENTIATION UNDER MICROGRAVITY

Cell differentiation is a progressive restriction of the developmental potential and increasing specialization of function which takes place during the development of the embryo and leads to the formation of specialized cells, tissues and organs**.** Microgavity conditions allow scientists to observe and explore phenomena and processes that are normally masked by the effects of Earth's gravity. NASA's microgravity biotechnology program focuses on three principal areas of research: protein crystal growth, mammalian cell and tissue culture, and fundamental biotechnology.

Results from the above research programs have demonstrated the benefits of using a low gravity environment for growing organic cells and tissues. Mammalian cells are very sensitive to growth conditions found in standard stirred bioreactors, because the fluid flow causes shear stress that discourage cell aggregation. This limits both the development of tissue and the degree to which it possesses structures and functions similar to those found in the human body (Duray et al, 1997)**.**

On Earth, most tissue cultures are grown in flat trays, but growing such tissues in reduced-gravity facilities has produced three-dimensional structures that are larger and more representative of tissues found in the human body (Freed et al., 1997; Goodwin et al., 1993). Given that better control of the stresses exerted on cells and tissues can play an important role in their culture, NASA scientists developed a rotating cell culture system (Figure 2.2 and Figure 2.3) that simulates microgravity environment.

Figure 2.2 The rotary cell culture system
A. 50 ml high aspect ratio vessel
B. 110 ml cylindrical cell culture vessel
C. 10 ml high aspect ratio vessel
D. Rotator base
E. Power supply and rotation speed controller

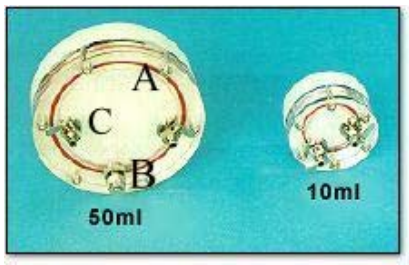

Figure 2.3 High aspect ratio vessel (HARV)
A. Peripheral screws
B. ¼ inch fill port
C. Luer lock syringe ports

Unlike most other culture systems that address one specific parameter such as shear stress at the expense of mass transfer of nutrients, metabolic wastes, three dimensionality and/or co-cultivation of dissimilar cell types, the RCCS is the first bioreactor designed to integrate simultaneously co-cultivation, low shear, high mass transfer and three-dimensional growth without sacrificing any other parameter (Tsao et al., 1997). Since its invention, scientists have successfully grown over 40 different cell types, including normal, cancerous, suspension and anchorage dependent cells. To date, no cell type tested has failed to grow in the RCCS.

The RCCS is a horizontally rotated, bubble free vessel with membrane diffusion gas exchange. Rotation inhibits the full effects of gravity and produces lower stress levels on the growing cells than previous experimental environments designed to facilitate tissue growth on Earth (Tsao et al., 1992). The culture medium, cells and cell aggregate particles rotate with the vessel and do not collide with the vessel walls or any other damaging objects under certain rotation speed. Destructive shear forces are minimized because this system has no impellers, air lifts, bubbles or agitators. Suspension cells or

anchorage-dependent cells on microcarrier beads establish a uniform, very low shear fluid suspension orbit within the vessels.

As the cell masses grow, the rotation speed is adjusted to compensate for increased sedimentation rates. The absence of damaging stress forces allows three-dimensional aggregation of large cell masses. The continuous rotation allows the tissue sample to be suspended in growth fluid and escape much of the influence of gravity.

Scientists at Johnson Space center are modifying the bioreactor, making it possible to automatically monitor and control levels of glucose, oxygen, pH and carbon dioxide in the solution containing the tissue. In the future, this technology will enable quicker, more through testing of larger numbers of drugs and treatments. Ultimately, the bioreactor is expected to provide a better simulation in comparison to the microgravity environment achieved in orbit.

CELLULAR AND MOLECULAR EFFECTS INDUCED BY MICROGRAVITY FORCES

Efforts to asses the neurobiological response to the space environment have been complicated by the considerable unknowns regarding the basic biological effects of space microgravity, particularly in relation to basic cellular functions and structures in eukariotes (Hughes-Fulford, 1993).

The majority of the gravitational studies to date indicate that cell regulatory pathways may be influenced by gravitational environmental changes (Vazquez, 1998). Typical neuroblastoma molecular and cellular responses involve gene activation and

expression leading to changes in cytoskeletal dynamics, trophic interactions and neurotransmitter levels (Hughes-Fulford and Lewis, 1996).

It is well known that altered gravity fields can modulate several cellular functions such as cell proliferation and differentiation. Possible molecular mechanisms that can explain these effects have been obtained in recent years indicating that gravity exerts its effect by modulating the expression of proto-oncogenes. Recent studies suggest that gravity may affect the intracellular signaling pathway activated by mitogenic stimuli such as growth factors, resulting in the modulation of proto-oncogene expression (Moore and Cogoli, 1996). Moreover, these results support the notion that microgravity can affect growth factor receptor-mediated signal transduction, possibly because of a gravity sensitive component in the cellular cytoskeleton and or different types of protein kinase (PKC)-mediated pathways (Cogoli, 1997). In addition, it has been postulated that the plasma membrane, which contains receptor and signal transduction proteins, is the interface between the proposed gravity sensitive intracellular cytoskeletal compartment and extracellular matrix compartment (Spooner, 1994).

Modern theories of cellular gravisensing mechanisms suggest a unifying model based on the concept that cells use tensegrity architecture to organize their cytoskeleton and stabilize their form (Ingber, 1997a). The postulated cell tensegrity architecture is composed of discrete cytoskeletal filamental networks that mechanically link specific cell surface receptors (integrins) to nuclear matrix scaffolds and to potential transducing molecules related to the cytoskeleton (Ingber, 1997b). It has been postulated that cells use tensegrity to respond to gravitational changes affecting cellular cytoskeleton, and thereby control cellular biochemistry and gene expression. These models of gravity sensing could

have important neurobiological consequences since the cytoskeleton and cell signal transduction pathways have been demonstrated to play a basic role in neural plasticity during development and maturity (Cambray-Deakin et al., 1991).

Information about tensegrity models is largely lacking in neurons. However, evidence for a direct connection between the cytoskeletal network and the extra cellular milieu mediated by integrins at adhesion sites has been reported (Jones, 1996). In the developing and mature central nervous system, the extracellular matrix provides a source of extrinsic cues to guide determination of cell fate, neuroblast migration, axon outgrowth and synapse formation. Modulation of the function of the cytoskeleton by gravity might, therefore, influence fundamental neural processes, and consequently have a high impact on neuronal functional and structural integrity.

Cytoskeletal proteins tagged with a green fluorescent protein were used to directly visualize the mechanical Pole of the cytoskeleton in determining cell shape (Heidemann, 1999). Rat embryo fibroblasts were deformed using glass needles either uncoated for purely physical manipulations, or coated with laminin to induce attachment to the cell surface. Cells responded to uncoated probes in accordance with a three-layer model in which a highly elastic nucleus is surrounded by cytoplasmic microtubules that behave as a jelly-like viscoelastic fluid. The third, outermost cortical layer is an elastic shell under sustained tension. Adhesive, laminin-coated needles caused focal recruitment of actin filaments to the contacted surface region and increased the cortical layer stiffness. This direct visualization of actin recruitment confirms a widely postulated model for mechanical connections between extracellular matrix proteins and the actin cytoskeleton. Cells tethered to laminin-treated needles strongly resisted elongation by actively

contracting. Whether using uncoated probes to apply simple deformations or laminin-coated probes to induce surface-to-cytoskeleton interaction, it was observed that experimentally applied forces produced exclusively local responses by both the actin and microtubule cytoskeleton. This local accommodation and dissipation of force is inconsistent with the proposal that cellular tensegrity determines cell shape.

DIFFERENTIATING NEUROBLASTOMA CELLS AS AN IN VITRO DEVELOPMENT MODEL

Neuroblastoma are believed to be precursors of the sympathetic ganglia derived from malignant tumors of the neural crest (Ishikawa, 1977), and have recently been shown to commonly arise from adrenal medulla (McGarry et al., 1988; Cooper et al., 1992). The cells may partially differentiate into cells having the appearance of immature neurons. The ability of many neuroblastoma cell lines to differentiate in response to a variety of biologic response modifiers has led to the use of neuroblastoma cell lines as model systems to study neuronal and neuroendocrine cell development and differentiation (Masters and Palsson, 1999). Neuroblastoma cells are considered excellent neuronal models of the peripheral nervous system since they exhibit morphological, biochemical and electrophysiological differentiation properties typical of in vivo neurons, when cultured and induced to differentiate as two-dimensional monolayers (Banker and Goslin, 1991).

THE BIOSYNTHESIS OF MAMMALIAN MELANIN

In vertebrates, melanins are synthesized in the melanosomes, subcellular granules in the cytoplasm of pigment cells (melanocytes). During embryogenesis, the immature melanocytes arise in the neural crest, migrate ventrally and make their way to predetermined areas of the skin where they complete the terminal stages of differentiation into the functional, mature melanocytes found in skin and hair follicles (Pawelek And Korner, 1982). In mammals, the melanocytes synthesize melanin in melanosomes and then transfer the pigmented melanosomes to keratinocytes, the most abundant cells of the skin.

The synthesis of melanin and possibly its transfer to keratinocytes can be simulated by a class of structurally related pituitary peptide hormones, referred to as melanocyte stimulating hormones (MSH) (Parkes and Vale, 1992). In mammals, tyrosinase activity and melanin synthesis are increased when melanocytes are exposed to MSH.

Darkening of the skin, as a result of this increased melanogenesis, can be observed in humans within 24 hours of injection of the MSH (Baker, 1994). The response is due not to the synthesis of melanin, but rather to the rapid transport of melanosomes from the center of the pigment cells out into the dendritic processes. The mechanism appears to involve an activation of the enzyme tyrosinase, as well as increase the rate of transfer of melanosomes to keratinocytes. Both processes appear to be regulated by intracellular increases in cyclic AMP, the “second messenger” of many peptide hormones (Bitensky et al, 1972).

The first measurable event following the binding of MSH to the receptor is a rapid rise in intracellular levels of cyclic AMP, occurring within a few minutes. A few hours later, there is an increase in tyrosinase activity, which is probably due to the removal of an inhibitor of tyrosinase rather than to the synthesis of new enzyme molecules. Tyrosinase is responsible for melanin biosynthesis. However, this question is not completely resolved, since at least one published report (Fuller and Hadley, 1979) claims that new molecules of tyrosinase are synthesized in response to MSH. The increase in tyrosinase activity is soon followed by a visible increase in melanin content in the cells. During this time the cells increase in size and extend long dendritic processes. Each of these events seems to be a response to elevated levels of cyclic AMP.

Recently, three factors regulating melanogenesis have been found, they are: dopachrome conversion factor, which accelerates the conversion of dopachrome into 5,6-dihydroxyindole; indole conversion factor, which accelerates the conversion of 5,6-dihydroxyindole into melanochrome; and indole blocking factor, which inhibits the conversion of 5,6-dihydroxyindole into melanochrome. Both dopachrome and indole conversion factors are associated with the tyrosinase isozymes found in melanosomes, and indole conversion factor appears to be synonymous to tyrosinase. These results indicate that regulation of the melanin biosynthesis pathway per se is highly complex.

PIGMENT CELLS

The formation of pigment in differentiating N1E-115 cells first observed by Dr. Marian Lewis of the Bioreactor Laboratory, Johnson Research Center (Huntsville, Alabama) was surprising and intriguing. It is well known that in vivo, the neural crest is a

pluripotent population of cells endowed with migratory capabilities. These cells spread throughout the embryo, settle in various locations and differentiate into a variety of derivatives (Bronner-Fraser etal, 1988; Newgreen et al, 1988; Morgan 1991). The derivatives include: the neurons and glial cells of the peripheral nevrous system, endocrine cells, melanocytes (pigment cells) and the so called mesectoderm, which plays a crucial role in formation of the connective and skeletal structure of the head (Le Douarin et al, 1993; Couly et al, 1993).

Mammalian melanocytes are neural crest-derived cells that synthesize the pigment melanin. These cells migrate from a central location to dermal-epidermal junctions early in gestation and situate themselves between keratinocytes of the basal layer of the epidermis, extending thin dendritic processes upwards into the epidermis.

The cytoskeleton of all eukaryotic cells is made up of tubulin-containing microtubules, actin-containing microfilaments and 10 nm intermediate filaments (Wolfe, 1993). Intermediate filaments are expressed in a tissue-specific manner, with vimentin expressed most commonly in cells of mesenchymal origin, desmin in muscle cells, three neurofilament proteins in neurons, glial fibrillar protein (GFAP) in glial cells (Steinert and Roop, 1988), and keratins in epithelial cells. It has been shown that the actin cytoskeleton plays an important role in both centripetal and centrifugal transport of pigment granules in the teleost retinal pigment epithelium (King-Smith et al., 1992). Cultured human melanocytes expressing vimentine genes and proteins under a variety of conditions have been demonstrated by using standard immunofluorecent, immunoblotting and northern blotting techniques (Si et al., 1993).

Lacour et al. (1992) have presented morphologic and histochemcial findings suggesting that dendrite outgrowth is regulated in a manner similar to neurite outgrowth, further emphasizing the common neural crest origin of neuronal and pigment cells. Given the common source of melanocytes and neuroblastoma cells, the transdifferentiation of neuroblastoma into melanocyte-like cells was considered plausible.

PRELIMINARY STUDIES

Based on the assumption that the differentiation of neuroblastoma cells in HRAV bioreactors would produce three dimensional tissue which more closely resembled the structure and function of the parental neural crest tissue, an experiment was initiated to replicate Dr. Marian Lewis's finding in the Cellular Bioengineering Laboratory. The objective was to confirm that cells would proliferate, undergo morphological differentiation, form viable three dimensional cell aggregates.

Briefly, the conclusions were as follows: 1) N1E-115 cells differentiating cells were successfully cultured in the HARV culture system; 2) as in plate cultures, differentiating murine cells detach off of microcarrier beads, however, in this case the cells formed three dimensional aggregates that remained metabolically active beyond 43 days; 3) differentiating cells formed neurite extensions on and across beads, that appeared to be making connections to other cells; 4) during the last three to four weeks, the cell clusters were dark orange and the sediment cells clusters appeared black. The contrast between nonpigmented and pigmented cells is shown in Figure 2.4.

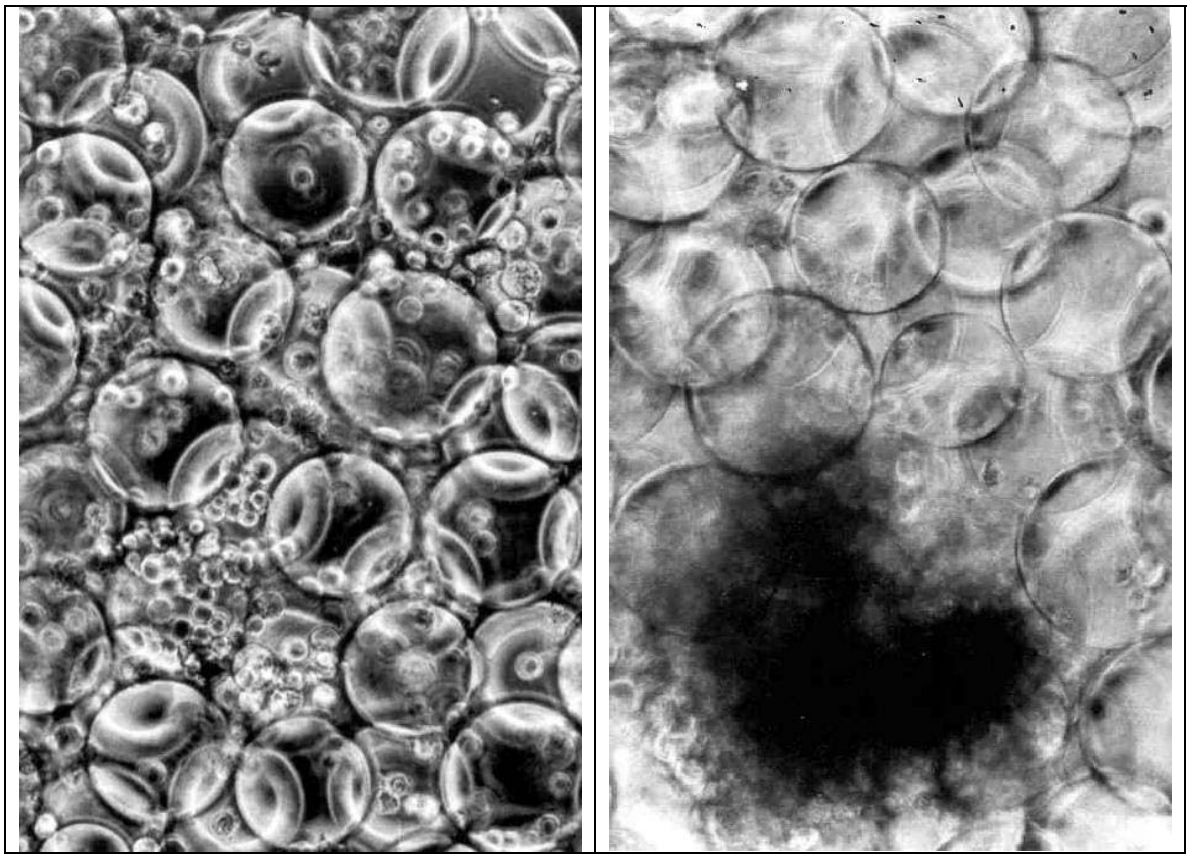

Figure 2.4 Black and white micrographs showing pigmented and nonpigmented cells: (a) Five days after culture in differentiation medium, cells are still attached to microcarrier beads; (b) A typical pigmented cell cluster, 24 days after culture in differentiating medium.

To confirm that the color was due to melanin. The pigment was extracted from cell aggregates following a published procedure (Harki et al, 1997). Briefly the bioreactor contents were centrifuged (500G, 10 min) and the pellet was washed twice with deionized water. The pellet was sonicated in 30 ml of 1M KOH for 10 min and the pigment was extracted from the cell debris by treatment with hot alkali (1M KOH at 100 ^{0}C for 3 hours) under reflux in an argon atmosphere. After filtration, the brown filtrate was acidified to pH 2 (7M HCl), and reacted with an oxidizing agent (100 μl 50% H_2O_2/ml). The pigment extracted from N1E-115 cells cultured in HARV bioreactors presented physical and chemical characteristics common to natural melanins previously

identified (Harki et al, 1997). The results are summarized in Table 2.1. Based on the similarity between the N1E-115 pigment and melanin, it was tempting to propose that N1E-115 pigment is melanin.

Table 2.1 Diagnostic tests for N1E-115 neuroblastoma pigment

Tests	N1E-115 pigment	Synthetic DOPA melanin (Harki et al, 1997)
Solubility in H_2O at 25 ^0C	-*	-
Solubility in 1 M KOH	+	+
Reaction to oxidizing agent: H_2O_2 (decolorization)	+	+
Precipitation by 7 M HCl (pH 2)	+	+

* + positive response; - negative response

OXYGEN AND DIFFERENTIATION

There are three kinds of oxygen supplies to cells and tissues---hypoxia, normoxia and hyperoxia. Hypoxia is a reduction of oxygen supply to cells and tissues below their physiological levels, and hyperoxia is increase of oxygen supply to cells and tissues above their physiological levels. In recent years, there has been an explosion of new information on the physiological and biochemical consequences of hypoxia and hyperoxia.

It is now clear that each of the organ systems --- heart, lungs, blood vessels and others, are affected by hypoxia in a somewhat different and unique manner. In particular, the lungs and blood vessels play a critical role in the body's defense against hypoxia. The eventual effect of hypoxia is on the heart and circulation (Arieff, 1992). Under conditions of tissue hypoxia, resulting from either hypoxemia or ischemia, oxidative phosphorylation is markedly reduced, and the glycolytic pathway becomes a relatively more important source of ATP synthesis (Apstein, 1992).

Dunn (2000) at Dartmouth College is one of the leading scientists investigating hypoxia adaptation of human disease models, using methods that non-invasively assess tumor hypoxia and perfusion. He is also using MR spectroscopy and imaging to study the metabolic responses of tumors to hypoxia/ischemia as well as radiation and chemotherapy.

Prabhakar et al. (1995) conducted experiments with phenochrocytoma-12 (PC-12), hepatoblastoma (Hep3B), neuroblastoma and fibroblast cells that were exposed either to normoxia (21%O_2) or to hypoxia (5%O_2) for one hour, after mRNAs for c-fos, c-jun, junB, junD were analyzed by northern blot assay. Increases in IERG (immediate early response genes) mRNAs were seen in PC-12, Hep3B and fibroblasts but not seen in neuroblastoma cells. Significant induction of c-fos mRNA was seen with hypoxic exposure as short as 15 min and the effects persisted for 10 h of low pO_2 exposure. These results demonstrated cell type selective mechanisms for c-fos promoter activation, and further observations suggest that increased IERG transcription is one of the early events in genomic adaptations to hypoxia. Voute (1995) reported that a very important factor in tumor treatment remains tumor hypoxia, while other factors such as metabolic factors also play a role.

Cornelissen (1997) pointed out that exposure of neuroblastoma cells to hyperbaric oxygen conditions enhanced the effects of meta-iodobenzylguanidine (a structural analogue of norepinephrine, used in its radio iodinated form for the diagnosis and therapy of neuroblastoma) on cell proliferation, lipid peroxidation and energy metabolism of the cell line. Cell proliferation and energy metabolism were decreased and lipid peroxidation was increased. Gendimenico (1990) reported that there are adverse effects of hyperbaric

oxygen on [^{3}H] uridine incorporation and uridine kinase activity in B104 rat neuroblastoma cells.

HYPOTHESIS

The following hypotheses were considered:

1) Microgravity is a factor in transdifferentiation of N1E-115 cells to melanocyte cells.
2) Hypoxia is a factor in transdifferentiation of N1E-115 cells to melanocyte cells.
3) Hypoglycemia is a factor in transdifferentiation of N1E-115 cells to melanocyte cells.

The third hypothesis was ruled out based on data from Dr. Lewis's laboratory, where color change was observed under well controlled glucose levels.

OBJECTIVES

We set out to test the remaining two hypotheses through the following specific objectives.

1) Replicate the transdifferentiation N1E-115 cells to pigmented cells with a goal of ruling out or confirming a role of simulated microgravity.
2) Investigate the effect of dissolved oxygen on N1E-115 cells in in vitro differentiation under normal and simulated microgravity.

REFERENCES

1. Apstein, C. S. 1992. Effects of ischemia, hypoxia and acidosis on cardiac systolic and diastolic function, and glycolytic metabolism in normal and hypertrophied hearts, In: Hypoxia, Metabolic Acidosis and the Circulation, 45-81. New York & Oxford: Oxford University Press.
2. Arieff, A. I. 1992. Hypoxia, Metabolic Acidosis and the Circulation, Preface. New York & Oxford: Oxford University Press.
3. Baker, B. I. 1994. Melanin-concentrating hormone updated-functional considerations. *TEM* 5:120-126.
4. Banker, G. and K. (Eds.) Goslin. 1991. *Culturing Nerve Cells* Cambridge, MA: MIT Press, pp11-109.
5. Bitensky, M. W.; H. B. Demopoulos and V. Russel. 1972. MSH-responsive adenyl cyclase in the Cloudman S-91 melanoma. *In Pigmentation: Its Genesis and Biological Control*, ed. V. Riley. 247-255. Appleton-Century-Crofts.
6. Bronner-Fraser, M. and S. E. Fraser. 1998. Cell lineage analysis reveals multipotency of some avian neural crest cells. *Nature* 335, 161-164.
7. Cambray-Deakin, M. A. 1991. *The Neuronal Cytoskeleton*, ed. R. D. Burgoyne, NewYork.
8. Cogoli, A. 1997. *ASGSB Bulletin* 10:5.
9. Cooper, M. J.; S. M. Steinberg and J. Chatten et al. 1992. Plasticity of neuroblastoma tumor cells to differentiate along fetal adrenal ganglionic lineage predicts for improved patient survival. *J. Clinical Investigation* 90:2402-2408.

10. Cornelissen, J.; A. B. P. VanKuilenburg and L. Elizinga et al. 1997. Hyperbaric oxygen enhances the effects of meta-iodobenzylguanidine (MIBG) on energy metabolism and lipid peroxidation in the human neuroblastoma cell line SK-N-BE (C). *Anticancer Research* 17:259-264.
11. Couly, G. F.; P. M. Coltey and N. M. Le Douarin. 1993. The triple origin of skull in higher vertebrates – a study in quail-chick chimeras. *Development*. 117, 409-429.
12. Dunn, J. F. 2000. http://www.dartmouth.edu/dms/physiol/faculty/dunn.html
13. Duray, P. H.; S. J. Hatfill and N. R. Pellis. 1997. Tissue Culture in Microgravity. *Science & Medicine*. 4(May/June):45-55.
14. Freed, L. E.; R. Langer and I. Martin et al. 1997. Tissue engineering of cartilage in space. *Medical Sciences* 94:13885-13890.
15. Fuller, B. B. and M. E. Hadley. 1979. Transcriptional and translational requirements for MSH of tyrosinase in melanoma cells. *Pigment Cell* 4:97-104.
16. Gendimenico, G. J. and N. Haugaad. 1990. Adverse effects of hyperbaric oxygen on [H-3] uridine incorporation and uridine kinase activity in B104 rat neuroblastoma cells. *Molecular and cellular biochemistry* 95:71-76.
17. Goda, F. G.; J. A. Bacic and O'Hara et al. 1996. The relationship between pO_2 and perfusion in to murine tumors after X-ray irradiation: a combined Gd-DTPA dynamic MRI and EPR oximetry study. *Cancer Research* 56:3344-3349.
18. Goodwin, T. J.; T. L. Prewett; D. A. Wolf and G. F. Spaulding. 1993. Reduced shear stress: A major component in the ability of mammalian tissue to form three-dimensional assemblies in simulated microgravity. *Journal of Cellular Biochemistry* 51:301-311.

19. Harki, E.; T. Talou and R. Dargent. 1997. Purification, characterization and analysis of melanin extracted from Tuber melanosporum Vitt. *Food Chemistry* 58:69-73.

20. Heidemann, S. R.; S. Kaech; R. E. Buxbaum et al. 1999. Direct observations of the mechanical behaviors of the cytoskeleton in living fibroblasts. *Journal of Cell Biology* 145:109~122.

21. Hughes-Fulford, M. 1993. Review of the biological effects of weightlessness on the human endocrine system. *Receptor* 3:145-154.

22. Hughes-Fulford, M. and M. L. Lewis. 1996. Effects of microgravity on osteoblast growth activation. *Experimental Cell Research* 224:103-109.

23. Ingber, D. E. 1997a. *ASGSB Bulletin* 10:49.

24. Ingber, D. E. 1997b. *Annu. Rev. Physiol.* 59:575.

25. Ishikawa, S. 1977. Differentiation of human neuroblastoma cells in vitro – morphological changes induced by dibutyryl cyclic AMP. *Acta Path. Jap.* 27:697-711.

26. Jones, L. S. 1996. Integrins: Possible functions in the adult CNS. *Trends Neurosci*. 19:68.

27. King-Smith, C. and P. Paz et al. 1997. Bidirectional pigment granule migration in isolated retinal pigment epithelial cells requires actin but not microtubules. *Cell motility and the cytoskeleton* 38:229-249.

28. Lacour, J. P.; P. R. Gordon and M. Eller et al. 1992. Cytoskeletal events underlying dendrite formation by cultured pigment cells. *J. Cellular Physiology* 151:287-299.

29. Le Douarin, N. M. and C. Ziller. 1993. Plasticity in neural crest cell differentiation. *Current Opinion in Cell Biology* 5, 1036-1043.

30. Masters, J. R. W. and B. Palsson. 1999. Volume 1: Cancer Cell Lines, In: *Human Cell Culture* 21-55. Dordrecht, Netherlands: Kluwer Academic Publishers.

31. McGarry, R. C.; A. Pinto, R. H. Hammersley-Straw et al. 1988. Expression of markers shared between human natural killer cells and neuroblastoma lines. *Cancer Immunol. Immunother* 27:47-52.

32. Moore, D. and A. Cogoli. 1996. In *Biological and Medical Research in Space,* ed. D. Moore, 1-106. Springer Verlag, Heidelberg.

33. Newgreen, D. and C. Erikson. 1986. The migration of neural crest cells. *International Review of Cytology* 103, 89-145.

34. Parkes, D. and W. Vale. 1992. Secretion of melanin-concentrating hormone and neuropeptide-EI from cultured rat hypothalamic cells. *Endocrinology* 131:1826-1831.

35. Pawelek, J. M. and A. M. Korner. 1982. The biosynthesis of mammalian melanin. *American Scientist* 70:136-145.

36. Lelkes P. 2000. University of Wisconsin Medical School. Private communication.

37. Prabhakar N. R.; B. C. Shneoy and M. S. Simonson et al, 1995. Cell selective induction and transcriptional activation of immediate early genes by hypoxia. *Brain Research* 697:266-270.

38. Si, S. P.; H. C. Tsou and X. Lee et al. 1993. Cultured human melanocytes express the intermediate filament vimentin. *J. Invest. Dermatol.* 110:383-386.

39. Spooner, B. S. 1994. Introduction-gravitational cellular and developmental biology. *J. Exp. Zool*. 269:177.

40. Stewards, R. P. and D. R. Roop. 1988. Molecular and cellular biology of intermediate filaments. *Ann. Rev. Biochem*. 57:593-625.

41. Tsao, Y. D.; S. R. Gonda and N. R. Pellis. 1997. Mass transfer characteristics of NASA bioreactors by numerical simulation. In Proc. *Advances in Heat and Mass Transfer in Biotechnology at The 1997 ASME International Mechanical Engineering Congress and Exposition,* BED-37: 69-73. ed. S. Clegg. Dallas, Texas, 16-21 November.

42. Tsao, Y. D.; T. J. Goodwin and D. A. Wolf. 1992. Responses of gravity level variations on the NASA/JSC bioreactor system. *The Physiologist* 35 (1 suppl):549-550.

43. Vazquez, M. E. 1998. Neurobiological problems in long-term deep space flights. *Adv. Space Res*. 22:171-183.

44. Voute P. A.; A. J. Vanderkleij and J. Dekraker et al. 1995. Clinical experience with radiation enhancement by hyperbaric oxygen in children with recurrent neuroblastoma stage IV. *European Journal of Cancer* 31A:596-600.

45. Voute P. A.; M. M. C. TielvanBuul and A. J. Vanderkleij et al. 1996. Combined I-131-MIBG therapy and hyperbaric oxygen therapy in children with recurrent neuroblastoma. *Journal of Nuclear Medicine* 37:1282-1282.

46. Wolfe, S. L. 1993. *Molecular and Cellular Biology*. Belmont, California: Wadsworth Publishing Company.

CHAPTER 3

GROWTH AND DIFFERENTIATION OF N1E-115 NEUROBLASTOMA CELLS IN HIGH ASPECT ROTATING VESSEL (HARV) UNDER HYPOXIA, NORMOXIA AND HYPEROXIA[1]

[1] Weicheng Zhang, William S. Kisaalita and Charles H. Keith. To be submitted to Biotechnology Progress. 12/2001.

ABSTRACT

Recent work from our laboratory involving the culture of differentiating murine neuroblastoma cells (N1E-115) in a High Aspect Rotation Vessel (HARV) bioreactor, has suggested a linkage between simulated microgravity and transdifferentiation of nerve-like N1E-115 neuroblastoma cells to pigmented (melanocyte-like) cells. The general purpose of this study was to confirm or rule out the possibility that the observed culture color change, from yellow to black/brown, was due to simulated microgravity and/or hypoxia. In this study, N1E-115 cells were cultured and differentiated on cytodex 3 beads in a HARV bioreactor under microgravity. Control cultures were differentiated under normal gravity in petri and tissue culture dishes. The culture vessels were operated in a CO_2 incubator at different incubator oxygen levels of hypoxia (10%), normoxia (18%) and hyperoxia (26%). pO2, pCO2 and pH were monitored with a blood gas analyzer (ABL5 Radiometer). Pigment formation was indirectly assessed by monitoring the activity of tyrosinase - a key enzyme in melanin synthesis. Tyrosinase activity was assayed with a standard stopped hydrazone 3-methyl-2-benzothiazoninone hydrazone (MBTH) method. It was not possible to replicate color development by differentiating neuroblastoma cells under simulated microgravity suggesting that the phenomena previously observed in our laboratory and by other investigations was not solely dependent on microgravity, if at all. Metabolic differences (O_2 consumption pattern) observed between cells differentiated under normal and microgravity were attributed more to O_2 mass transport limitation into the HARV. Also, hopoxia was not proven to be a factor in transdifferentiation of N1E-115 neuroblastoma cells to melanocyte-like cells.

INDEX WORDS: N1E-115 Neuroblastoma cell, cell differentiation, microgravity, High Aspect Rotation Vessel (HRAV), hypoxia, normoxia, hyperoxia, pigment cell, tyrosinase.

INTRODUCTION

Manned space exploration plans for the next century include a piloted mission to Mars. However, for such a mission, humans must be protected against the harsh environment of space, in particular, against the hazards of microgravity. When humans are exposed to the conditions of outer space, a number of neurologic disorders emerge. These pathological changes affect a variety of neural systems ranging from motor to sensory functions, and the effects can be long lasting. However, the nature of the functional and structural mechanisms underlying these changes is unknown. It is becoming more and more important to advance our scientific understanding of how biological processes are affected by microgravity.

In preliminary experiments conducted by Dr. Marian Lewis at the Bioreactor Laboratory, Johnson Research Center, Huntsville, Alabama, N1E-115 neuroblastoma cells were observed to change color when differentiated under simulated microgravity after 8 to 10 days of exposure to differentiating medium. These observations were replicated in our laboratory, N1E-115 cells differentiated under simulated microgravity exhibited a color change from yellow to brown/black during approximately the same period of 8 to 10 days. These qualitative observations seemed to suggest the possibility of transdifferentiation of N1E-115 cells to pigmented cells in response to microgravity. A similar phenomenon has been observed in the laboratory at the Department of Medicine, the University of Wisconsin Medical School with PC12 and other neuroblastoma cells. The color change was attributed to hypoxia (insufficient oxygen supply) and hypoglycemia (insufficient glucose feeding) or improper handling of the culture (Lelkes, personal communication, 2000).

The original goal of this study was to confirm or rule out the possibility that the observed color change was due to simulated microgravity. In a preliminary experiments, N1E-115 cells were cultured and differentiated on cytodex beads in a High Aspect Rotating Vessel (HARV) bioreactor (simulated microgravity) and on cytodex beads in petri dishes (normal gravity), as well as in tissue culture dishes without beads (normal gravity). The bioreactors were operated in a CO_2 incubator at normal oxygen levels (normoxia). Care was taken to maintain sufficient glucose by frequently refreshing the medium. The previously observed color change was not replicated in these experiments.

Most of the literature on oxygen and neuroblastoma cells is concerned with using hypoxia and hyperbaric oxygen to treat neuroblastoma tumors (e.g., Cornelissen et al, 1997, Voute et al, 1995 and 1996, Goda et al, 1996). This suggests that changing dissolved oxygen may play a role in neuroblastoma cell differentiation, however, no reports were found specifically addressing the transdifferentiation of neuroblastoma cells.

The general hypothesis in this study was that microgravity, hypoxia and hypoglycemia are key factors in the transdifferentiation of N1E-115 neuroblastoma cells into pigmented cells. The hypoglycemia hypothesis was considered unlikely based on the previous data from Dr. Lewis's laboratory where color change was observed under well controlled glucose levels. The current research focus in the Cellular Bioengineering Laboratory is the development of cell-based systems with applications in accelerated drug discovery. In light of this, the motivation to pursue N1E-115 transdifferentiation was based on two potential benefits. First, understanding transdifferentiation of neuroblastoma into melanocyte-like cells may provide a convenient experimental system with which to determine the influence of microgravity on the development of neural crest

and/or other nervous system cells in vitro and possibly in vivo. Second, the system has the potential to provide an in vitro melanoma model, which could lead to the determination of intracellular targets and elucidation of the transduction pathway.

MATERIALS AND METHODS

Cell line and cell culture. Murine neuroblastoma cells (N1E-115) were obtained from Dr. M. Nirenberg of the National Institute of Health. A previously published protocol (Kimhi et al., 1976) was followed. Briefly, N1E-115 cells were grown to confluence in a 75 cm^2 T culture flask in growth medium containing 1.34% Dulbelcco's Modified Eagle Medium (DMEM, GIBCO), 0.37% $NaHCO_3$, 13% Fetal Bovine Serum (FBS, HYCLONE) and 1% Penicillin-Streptomycin (Pen-Strep, GIBCO). The culture was maintained in a CO_2 water-jacketed incubator (Forma Scientific) whose temperature was controlled at 37 ^oC, humidity greater than 90% and CO_2 at 10%. The medium was changed when the color of the medium turned orange/yellow.

Cytodex 3 bead conditioning. 0.8g dry Cytodex® 3 beads were weighted out and put into a 50 ml centrifuge tube containing 40 ml Calcium/Magnesium Free (CMF) PBS. The beads were suspended and placed at room temperature for 3 hours to swell. The supernatant buffer was aspirated and fresh CMF-PBS was added. The above washing steps were repeated at least twice. Then the beads in fresh CMF-PBS were sterilized by autoclaving (115^0C for 15 min at 15 psi). The beads were rinsed using fresh culture medium and then resuspended in 40 ml fresh culture medium.

N1E-115 Cell differentiation under hypoxia, normoxia and hyperoxia. Confluent cells were removed from the T flasks using a cell scraper and counted, and then

inoculated into HARVs, petri and tissue culture dishes with the appropriate number of beads (Table 3.1). On the 2nd day, growth medium was replaced by differentiation medium composed of 1.34% DMEM, 0.37% $NaHCO_3$, 0.5% FBS and 1% Pen-Strep. Differentiation medium was changed at the 2nd, 4th and 8th days during the 12 day differentiation period. The incubator O_2 was monitored and controlled at 10%, 18% or 26% with an Oxygen Controller (PROOX Model 110, Reming Bioinstruments Co.). The three culture vessels were maintained in the CO_2 incubator at 37 ^{0}C, 90% relative humidity and 10% CO_2. The rotation speed of bioreactor HARV was controlled at 13 rpm.

pH, pCO_2, pO_2 Analysis. The media from the culture vessels was analyzed for pH, pCO_2, pO_2 with a commercial blood analyzer (ABL5, Radiometer America, Inc.). ABL5 was activated from standby state and calibrated automatically. To obtain the most accurate results, a 3 to 4 ml media sample was taken from each of the culture vessels using a syringe and immediately injected into the ABL5 for analysis. The analytical results were printed out after a couple of minutes.

Glucose measurement. A 3 ml sample was centrifuged and filtered, the glucose concentration was measured following a standard lab protocol with a HPLC (Model: SCL-6B, Shimadzu). The HPLC set up was as follows. Column: Corgel 64H (Transgenomic, L=300nm, ID=7.8mm); Eluant: 4 mN H_2SO_4; Flow Rate: 0.6 ml/min; Oven temp: 60^{o}C; Run time: 30 min.

Protein assay. The Bio-Rad Detergent Compatible (DC) Protein Assay Kit II (reagent A, S, and B) and Protocol were followed. Briefly, 5 dilutions of BSA standard containing 23.8 - 214.5 μg/ml proteins were prepared each time the assay was performed. For best

results, the standards were prepared in the same buffer (containing 200µl protease inhibitor cocktail per 2 ml) as the sample. A detergent buffer was made of 20 mM pH7.5 potassium phosphate buffer containing 0.5% (v/v) Triton-100. Cells and/or beads were centrifuged (500g, 4 ^{0}C for 10 min). The supernatant was removed and cells were re-suspended by vortexing in 2ml detergent buffer with 200 µl proteinase inhibitor cocktail for 5 min. The extract was twice centrifuged (9000g, 4 ^{0}C for 15 min). The supernatant was frozen at -20 ^{0}C for future measurement. Standards and samples were aliquoted into a 96 well microtiter plate and the absorbances were measured at 750 nm using a MRX Microplate Reader (DYNEX Technologies Inc.).

Standard stopped hydrazone 3-methyl-2-benzothiazoninone hydrazone (MBTH) tyrosinase assay. A method previously published by Winder (1994) and Winder et al. (1991) was followed. To prepare samples, cells were re-suspended by vortexing in 2 ml detergent buffer and sonicated in ice water for 30 s (Branson 1200 Sonicate machine, 5 µm setting). The extracts was centrifuged (9000g, 4 ^{0}C for 15 min) twice. The final supernatant was dialyzed against 20 mM potassium phosphate (pH7.5) (1 liter for 1 h, then 4 liter overnight). The sample was frozen at -20 ^{0}C for measurement for later analysis. The assay buffer was made as follows: 100 mM pH7.1 potassium phosphate, 4% (v/v) N, N'-dimethylformamide (Aldrich) and 0.1% (v/v) Triton X-100. The detergent buffer was made as follows: 20 mM pH7.5 potassium phosphate, 0.5% (v/v) Triton-100, protease inhibitor cocktail 200µl per 2 ml. The pre-reaction mixture was made as follows: 470 µl reaction mixture containing 250 µl of assay buffer, 100 µl of 5 mM L-dopa (Sigma), 120 µl of 25 mM MBTH (Sigma). To generate the tyrosinase activity calibration curve, 0 to 20 µl of 10 µg/ml tyrosinase and 106 to 126 µl of detergent

buffer were mixed in eppendorf tube to a final volume of 610 ml, yielding a final enzyme concentration range of 0.07 – 0.33 μg/ml. For sample analysis, 140 μl of sample was added to 470 μl of pre-reaction mixture and incubated at 37 ^{0}C for 10 min. The reaction was stopped by adding 500 μl of 1 M perchloric acid (Fluka). Then the mixture was centrifuged (9000g, 5 min) at room temperature. 350 μl supernatant was directly transferred to a 96 well microtiter plate and the absorption was measured at 490nm with a MRX Microplate Reader (DYNEX Technologies, Inc.).

RESULTS AND DISCUSSION

Transdifferentiation of N1E-115 cells.

The color change previously observed with N1E-115 cells differentiated in HARV vessel was not replicated in our laboratory. The rationale for monitoring tyrosinase activity was based on the fact that tyrosinase is responsible for melanin biosynthesis and the increase in tyrosinase activity is usually followed by a visible increase in melanin content in the cells (Fuller et al, 1979). Tyrosinase analysis results are presented in Table 3.2. As shown, no tyrosinase activity was found from cells in the tissue culture vessel, however, there was activity in the HARV and petri dish – cultured cells. These activity were attributed to interferences from beads. The supernatant from beads incubated in HARV for 12 days without cells exhibited tyrosinase activity of 11.9 units, which approached the activities found in HARV and petri dish with cells. The inability to replicate color development by differentiating neuroblastoma cells under simulated microgravity suggested that the phenomena in previous experiments was not solely dependent on microgravity, if at all. The previous color change might have been

due to the presence or absence of growth factors in fetal bovine serum, since changes have been implemented by Hyclone in the way FBS used in processed between the FBS batches in our first and second sets of experiments.

Morphological differentiation and protein recovery at the end of differentiation.

The trigger for N1E-115 differentiation was the extremely low serum in differentiation medium. Cells were expected to be induced to differentiate in response to the lack of growth factors in the differentiation medium while maintaining sufficient glucose feeding. N1E-115 cells were morphologically differentiated in the three culture vessels. In the tissue culture dishes, the long outgrowth neurites and elongated cells were formed after 1 or 2 days of differentiation, and fully initiated after 4 or 5 days. In HARV and petri dishes (both with beads), a few cells formed neurites across the beads after 3 to 4 days. By the 11^{th} day of culture in differentiation medium, the neurites were visible in the petri dishes but not in the HARV. Figure 3.1 shows the morphological characteristics before and after differentiation under the three culture conditions.

The cytodex 3 beads used in HARV (Figure 3.2) and the petri dishes are the preferred microcarrier for cells known to be difficult to culture in vitro. They are formed by chemically coupling a thin layer of denatured collagen to the cross-linked dextran matrix. The resulting average microgravity experienced by these beads in HARV has been calculated to be about 0.01g (Radin et al, 2001). Viscous coupling enables the liquid inside to accelerate until the entire fluid mass is rotating at the same angular rate as the outside wall. Microcarrier beads and cells in this environment obey simple kinematics and are uniformly suspended in the fluid at a 13 rpm rotational speed. At this speed, no collisions are experienced by the microcarrier with the outer wall of the vessel. The

relative motion between the microcarriers/cells and the fluid medium offers great advantages for mass transfer in the HARV (Gao et al., 1997). N1E-115 cells were observed well attached to the beads and actually formed three-dimensional aggregates of cells/beads within the first few hours to 24 hours in HARV. The differences in morphology may be attributed to enhanced opportunities for cells to form 3-dimensional aggregates in HARV due to the presence of beads.

In both the petri dishes and the HARV, cells aggregated on beads as shown in Figure 3.1b, however, cells began to detach from beads, especially in HARV. Until differentiation day 5 or 6, very few cells remained on the bead surface in HARV. Differentiating N1E-115 cells have been shown to exhibit differentiation-associated cell detachment (Kisaalita and Bowen, 1995), which may partly explain the above observation. More importantly, although the relative motion between particles and the fluid enhances mass transfer, the shear stress on the microcarriers was probably sufficient to contribute to the separation of the cell clusters from the beads. In the petri dishes, the cell aggregates remained attached to the beads, probably because of the vessel's static nature.

Protein recovery (ratio of protein before and after differentiation) at a standard incubator oxygen level of 18% was higher than that at hypoxic and hyperoxic incubator oxygen levels of 10% and 26% respectively (Table 3.3). Hypoxia and hyperoxia probably lead to oxygen deprivation and oxidative damage, respectively, altering N1E-115 cell metabolism (Sahai et al, 1989; Heaocock et al, 1990) which may lead to more cell death. Tissue culture dishes yielded the highest protein recovery suggesting differences in tissue formed between the culture vessels used.

O_2 consumption pattern.

The HARV and petri dish vessels were inoculated with the same cell density of 1.2 x 10^5 cells/ml to allow comparison of O2 consumption pattern during differentiation. The steady state dissolved O_2 and CO_2 in the 3 culture vessels, without cells, were initially established and the results are presented in Table 3.4. To compare the dissolved O_2 consumption patterns, differences between the measured O_2 and CO_2 (pO_2 and pCO_2) and the steady state no-cell values were calculated and are presented in Figure 3.3a for culture conditions of normal incubator settings (37^0C, 90% relative humidity, 10% CO_2 and 18% head space O_2). As shown in Figure 3.3a, HARV exhibited a larger difference in pO_2 when compared to the petri dish. A similar phenomenon was observed under hypoxia and hyperoxia (Figure 3.3b). A possible interpretation was that N1E-115 cells in HARV had higher cellular activity and consumed more oxygen during the differentiation process. But the pCO_2 difference (Figure 3.3c and 3.3d) did not provide strong evidence in support of higher cellular activities in HARV. The fact that pCO_2 differences (18% O_2 level vs 10% O_2 level, Pr = 0.0001; 18% O_2 level vs 26% O_2 level, Pr = 0.0001) in HARV were a little bit higher in the first several days, suggested slightly higher cellular activities during this period in HARV at the hypoxia (10%) and hyperoxia (26%). However, most pCO_2 differences were below zero. Combining the above observations, strongly points to limitations in HRAV oxygen transportation from the incubator to the inside of the reactor and CO_2 transportation from the inside of the reactor to the incubator. Lower HARV steady state dissolved pO_2 and pCO_2, without cells, presented in Table 3.4 and lack of differences in glucose consumption pattern, across those culture vessels presented in Figure 3.6, further confirmed this point. Also, in comparison to a petri dish, it took 3 to 4

times longer for dissolved CO_2 equilibration in the HARV vessel under 10% CO_2 incubator environment, further attesting to limited transport characteristics of the vessel. The test was conducted with an aqueous solution of phenol red at 30 mg/L.

Oxygen is often the first component to become rate limiting because of relatively high cell requirements for oxygen and its low solubility in the fluid medium (Kleis, 1997). In comparison to the stationery culture, oxygen mass transfer in HARV is enhanced due to the relative motion of microcarrier beads (Gao et al, 2001), which was probably responsible for a higher O_2 consumption by the cells during the first half of the culture period in HARV. The fact that the pO_2 difference was larger in HARV points to diffusion of O_2 through the membrane of the vessel as limiting, although the incubator air is circulated through the oxygenation membrane by the external air pump at about 1liter/min, providing an oxygen-rich environment at the oxygenation boundary. The cell-O_2 demand was not being met. This is further confirmed by the results presented in Figure 3.3e, that an increase of the incubator oxygen level resulted in an increased O_2 difference across the three culture vessels. The reduction in pO_2 differences after 3 to 5 days of differentiation was attributed to either change in metabolism or cell death, confirmed with trypan blue stain.

Morphological effects due to oxygen levels were only observed from tissue culture dish cells during the first two days of differentiation. As shown in Figure 3.4, cells at 26% O_2 exhibited a unique morphology. According to the literature, hypoxia impairs cell fusion and differentiation process in human cytotrophoblasts, in vitro (Alsat, et al., 1996). Morphological differentiation of mouse neuroblastoma cells was accompanied by an increase in oxygen consumption (Nissen, et al., 1973). Which can be

interpreted to mean that higher-levels of oxygen supply will promote cell differentiation and lower levels will impair differentiation. On the contrary, the unique morphology in Figure 3.4 (e and f) did not manifest in any observable morphological differentiation differences later.

Incubator oxygen level changes from 10% to 26% did not significantly affect pH in the three culture vessels with the exception of hyperoxia in petri dish. The pH ranged between 6.5 to 7.3 (Figure 3.5), well within the physiological range for the culture.

Medium was changed on the 2^{nd}, 4^{th} and the 8^{th} day during the differentiation process. Based on glucose analysis (Figure 3.6), glucose feeding rate was sufficient to maintain cell metabolism. The glucose dropped rapidly during the first two days, confirming a higher metabolic activity of the cells across the three culture vessels. The cells were metabolizing glucose in the later phase due to a combination of slowed metabolism and cell death.

CONCLUSIONS

In conclusion, it was not possible to replicate color development by differentiating neuroblastoma cells under simulated microgravity suggesting that the phenomena previously observed in our laboratory and by other investigations was not solely dependent on microgravity, if at all. Metabolic differences (O_2 consumption pattern) observed between cells differentiated under normal and microgravity were attributed more to O_2 mass transport limitation into the HARV. Also, hopoxia was not proven to be a factor in transdifferentiation of N1E-115 neuroblastoma cells to melanocyte-like cells.

ACKNOWLEDGEMENTS

The authors would like to acknowledge Dianne Stroman and Melissa Bishop for their technical support of this work, and Sarah Lee for glucose analysis.

REFERENCES

1. Alsat, E.; P. Wyplosz; A. Malassine; J. Guibourdenche and D. Evain-brion. Hypoxia impairs cell fusion and differentiation process in human cytotrophoblast, in vitro. *Journal of Cellular Physiology* **1996**, 168, 346-353.
2. Cornelissen J.; A. B. P. VanKuilenburg; L. Elizinga. Hyperbaric oxygen enhances the effects of meta-iodobenzylguanidine (MIBG) on energy metabolism and lipid peroxidation in the human neuroblastoma cell line SK-N-BE (C). *Anticancer Research* **1997**, 17, 259-264.
3. Fuller B. B.; M. E. Hadley. Transcriptional and translational requirements for MSH of tyrosinase in melanoma cells. *Pigment Cell* **1979**, 4, 97-104.
4. Gao, H.; P. S. Ayyaswamy; P. Ducheyne and S. Radin. Surface transformation of bioactive glass in bioreactors simulating microgravity conditions. Part II: Numerical simulations. *Biotechnology and Bioengineering* **2001**, 75, 379-385.
5. Gao, H.; S. P. S. Ayyaswamy and P. Ducheyne. Numerical simulation of global diffusive mass transfer in a rotating wall vessel bioreactor. In Proc. *Advances in Heat and Mass Transfer in Biotechnology – 1997,* at The 1997 ASME International Mechanical Engineering Congress and Exposition. **1997**, BED-37: 59-67. ed. Scott Clegg. Dallas, Texas, November 16-21.

6. Goda F; G. Bacic; J. A. O'Hara. The relationship between pO_2 and perfusion in to murine tumors after X-ray irradiation: a combined Gd-DTPA dynamic MRI and EPR oximetry study. *Cancer Research* **1996**, 56, 3344-3349.
7. Heacock, C. S.; R. M. Sutherland. Enhanced synthesis of stress proteins caused by hypoxia and relation to altered cell growth and metabolism. Br. J. Cancer. **1990**, 62, 217-215.
8. Kimhi. Y; C. Palfrey; I. Spector; Y. Barak; U. Z. Littauer. *Proc. Natl. Acad. Sci. U.S.A.* **1976,** 73, 462-466.
9. Kisaalita, W. S. and J. M. Bowen. Effect of culture age on the susceptibility of differentiating neuroblastoma cells to retinoid cytotoxicity. *Biotechnology and Bioengineering* **1995**, 50, 580-586.
10. Kleis, S. J. Mass transport considerations for microgravity cell cultures in the NASA/JSC bioreactor. In Proc. *Advances in Heat and Mass Transfer in Biotechnology – 1997,* at The 1997 ASME International Mechanical Engineering Congress and Exposition. **1997**, BED-37: 49-57. ed. Scott Clegg. Dallas, Texas, November 16-21.
11. Lelkes P. University of Wisconsin Medical School. Private communication. **2000**.
12. Nissen, C.; J. Ciesielski-Treska; L. Hertz and P. Mandel. Regulation of oxygen consumption in neuroblastoma cells: Effects of differentiation and of potassium. *Journal of Neurochemistry* **1973**, 20, 1029-1035.
13. Radin, S.; P. Ducheyne; P. S. Ayyaswamy and H. Gao. Surface transformation of bioactive glass in bioreactors simulating microgravity conditions. Part I: Experimental Study. *Biotechnology and Bioengineering* **2001**, 75, 369-378.

14. Sahai, A.; G. Xu; R. S. Sandler; R. L. Tannen. Rocking promotes differentiated properties in LLC-PK1 cells by improved oxygenation. *Am. J. Physiol.* **1989**, 256(Cell Physiol., 25), C1064-C1069.

15. Voute P. A.; A. J. Vanderkleij; J. Dekraker. Clinical experience with radiation enhancement by hyperbaric oxygen in children with recurrent neuroblastoma stage IV. *European Journal of Cancer* **1995**, 31A, 596-600.

16. Voute P. A.; M. M. C. TielvanBuul; A. J. Vanderkleij. Combined I-131-MIBG therapy and hyperbaric oxygen therapy in children with recurrent neuroblastoma. *Journal of Nuclear Medicine* **1996**, 37, 1282-1282.

17. Winder A. J. A stopped spectrophotometric assay for the dopa oxidase activity of tyrosinase. *Biochem. Biophys. Methods* **1994**, 28, 173-183.

18. Winder A. J.; H. Harris. New assays for the tyrosine hydroxylase and dopa oxidase activities of tyrosinase. *Eur. J. Biochem.* **1991**, 198, 317-326.

Table 3.1 Cytrodex 3 beads and neuroblastoma cell inoculation of the culture vessels

Attribute	Culture vessel		
	HARV (with beads)	Petri dish (with beads)	Tissue Culture dish (without beads)
Cells inoculated (number of cells)	6×10^6	1.8×10^6	0.52×10^6
Beads Added (number of beads)	7.5×10^5 (10 ml)	2.25×10^5 (3 ml)	---
Final working volume (ml)	50	15	15

Table 3.2 Tyrosinase activity analysis results before and after 12 days of culture in differentiation medium

Culture vessel	Tyrosinase activity (Unit*)						
	Before differentiation (cells without beads)	After 12 days of culture in differentiation medium					
		Hypoxia (10% O_2)		Normoxia (18% O_2)		Hyperoxia (26% O_2)	
HARV	0	A#	9.59	A	15.00	A	12.47
	0	B	7.95	B	12.60	B	10.69
Petri dish	0	A	5.69	A	8.22	A	12.54
	0	B	4.38	B	10.07	B	11.37
Tissue culture dish	0	A	0	A	0	A	0
	0	B	0	B	0	B	0

* 1 Unit corresponds to the amount of enzyme required to increase the absorbance at 305 nm by 0.001 per minute at pH 6.5 and 25^0C (L-tyrosine as substrate, 3.0 ml mixture); 30 absorbance-U as described above are equivalent to ~ 1 U (when 1 U is the amount of enzyme which oxidizes 1 μmol 4-methylcatechol per minute at pH 6.5 and 25^0C).
# A & B were parallel experiments.

Table 3.3 Protein recovery after differentiation

Incubator O_2 level (v/v)	Culture vessel		
	HARV	Petri dish	Tissue culture dish
Hypoxia, 10%	18.5%	38.7%	47.2%
Normoxia, 18%	28.5%	51.3%	63.1%
Hyperoxia, 26%	25.6%	45.4%	54.8%

Table 3.4 The steady state (over night) dissolved pO_2 and pCO_2 of differentiation medium in different culture vessels without cells

Oxygen level	HARV		Petri dish		Tissue culture dish	
	pO_2 (mmHg)	pCO_2 (mmHg)	PO_2 (mmHg)	pCO_2 (mmHg)	pO_2 (mmHg)	pCO_2 (mmHg)
10%	101	71	109	71	110	73
18%	131	70	141	63	137	75
26%	173	69	184	69	180	72

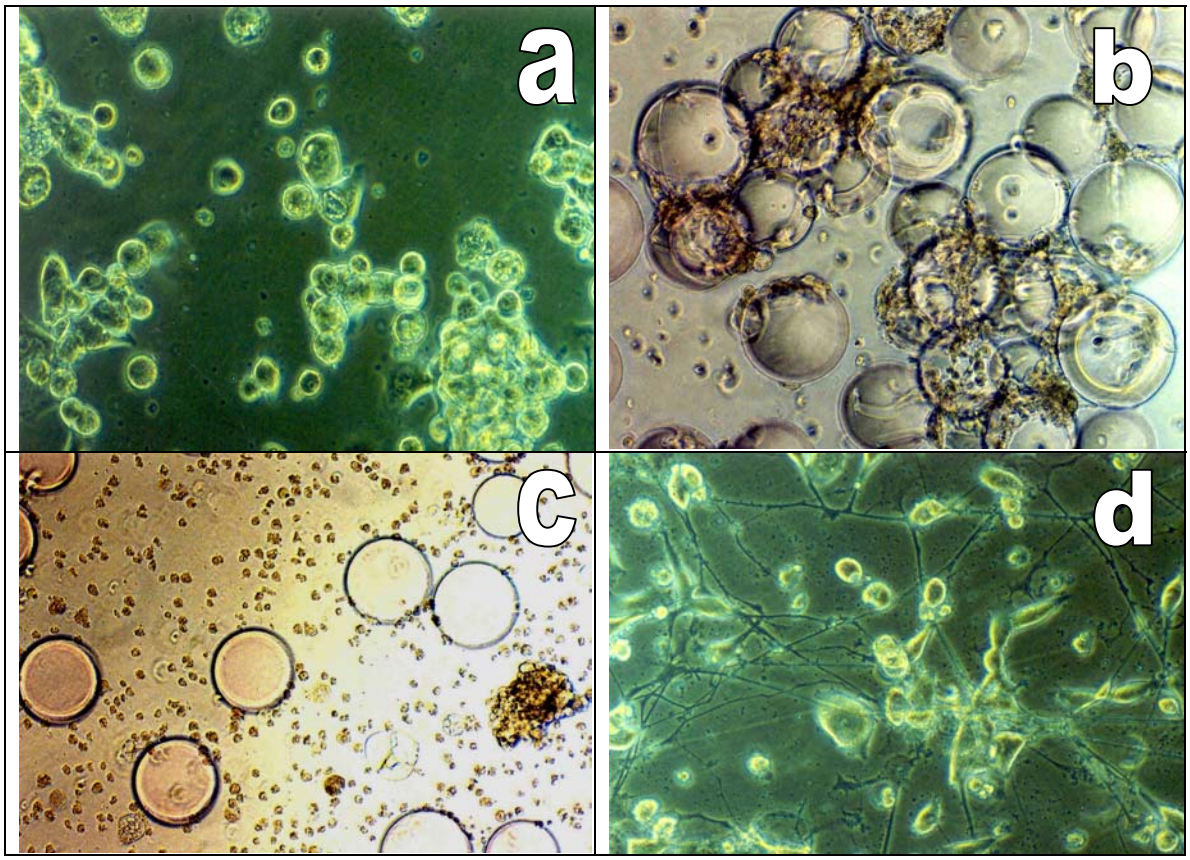

Figure 3.1 Photographical images of N1E-115 cells differentiated at incubator oxygen level of 10%. (a) Before differentiation; (b) After 11 days in HARV (with beads); (c) After 11 days in a petri dish (with beads); (d) After 11 days in a tissue culture dish (without beads). Bead diameter is approximately 175 μm.

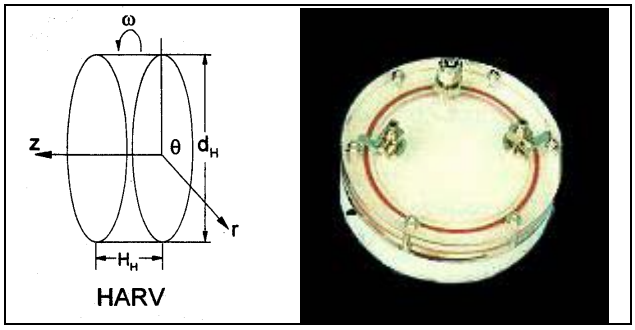

Figure 3.2 Schematic of the High Aspect Rotating Vessel (HARV).
The 50 ml HARV is a cylindrical vessel of diameter $d_H \approx 10$ cm, and height $H_H \approx 0.64$ cm, and was filled completely with 50 ml solution. When operating, it rotates about its horizontal z-axis at $\omega = 13$ rpm, an air pump draws incubator air through a filter and discharges it through the oxygenator membrane of the culture chamber.

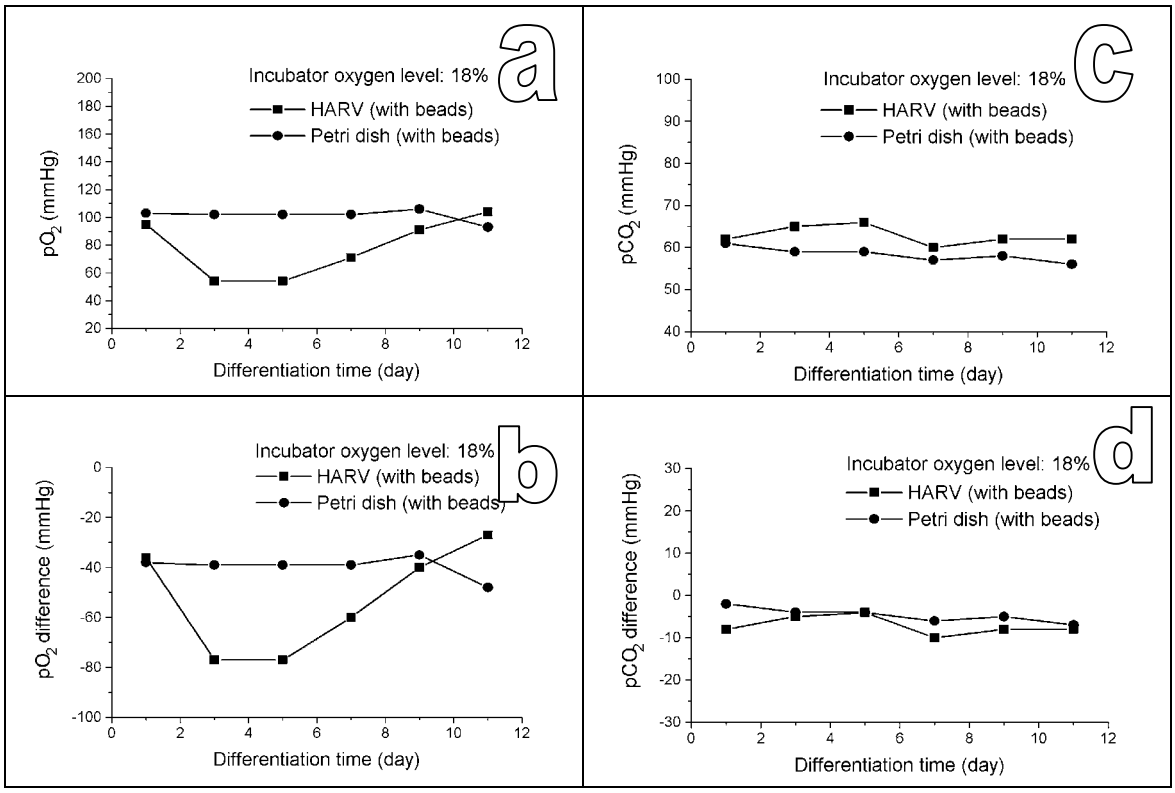

Figure 3.3a Comparison of pO_2 and pCO_2 differences in HARV and petri dish under culture conditions of normoxia. pO_2 and pCO_2 differences were calculated by subtracting the steady state dissolved O_2 and CO_2 (without cells) from the measured dissolved O_2 and CO_2, respectively. Statistical comparison (GLM procedure in SAS software package) of the plots returned the following results: a) HARV pO_2 vs petri dish pO_2 (Pr =0.0001); b) HARV pO_2 difference vs petri dish pO_2 difference (Pr =0.0011); c) HARV pCO_2 vs petri dish pCO_2 (Pr =0.0011); and d) HARV pCO_2 difference vs petri dish pCO_2 difference (Pr =0.0094).

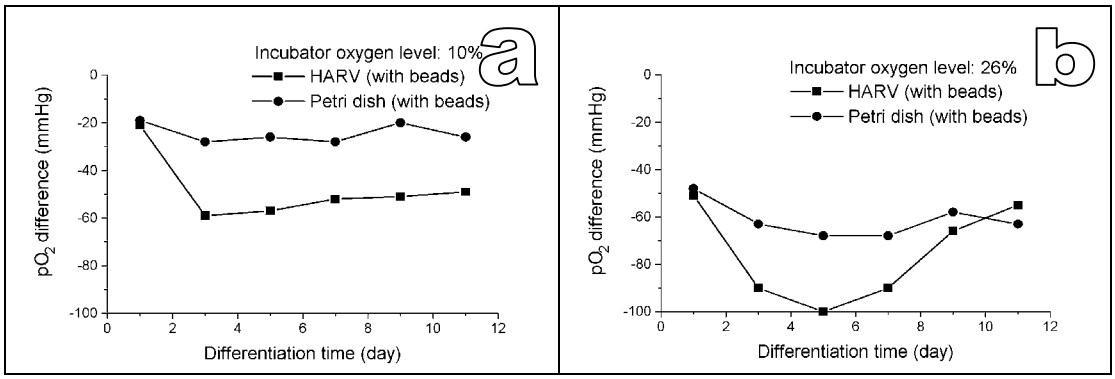

Figure 3.3b Comparison of pO_2 differences in HARV vs petri dish under culture conditions of hypoxia (10%) and hyperoxia (26%). pO_2 differences were calculated by subtracting the steady state dissolved O_2 (without cells) from the measured dissolved O_2. Statistical comparison of pO_2 differences (GLM procedure in SAS software package) of the plots returned the following results: a) HARV vs petri dish under hypoxia (Pr =0.0001); b) HARV vs petri dish under hyperoxia (Pr =0.0001).

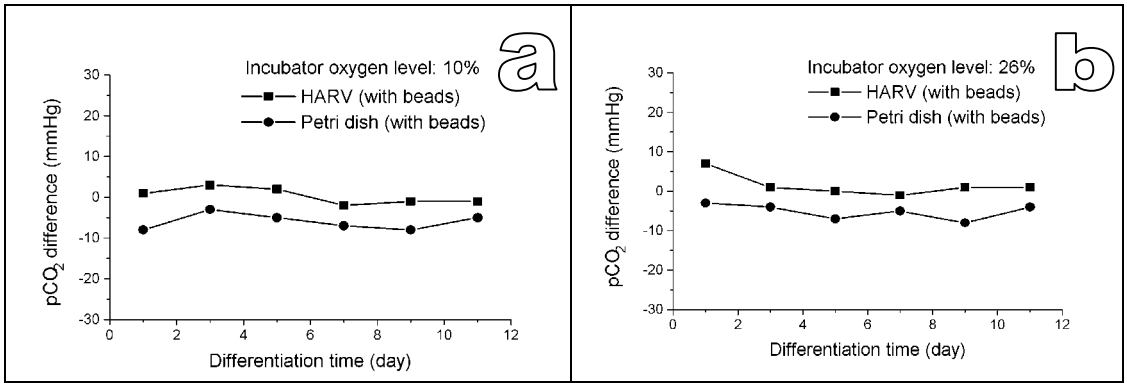

Figure 3.3c Comparison of pCO_2 differences in HARV vs petri dish under culture conditions of hypoxia (10%) and hyperoxia (26%). pCO_2 differences were calculated by subtracting the steady state dissolved CO_2 (without cells) from the measured dissolved CO_2. Statistical comparison of pCO_2 differences (GLM procedure in SAS software package) of the plots returned the following results: a) HARV vs petri dish under hypoxia (Pr =0.0001); b) HARV vs petri dish under hyperoxia (Pr =0.0001).

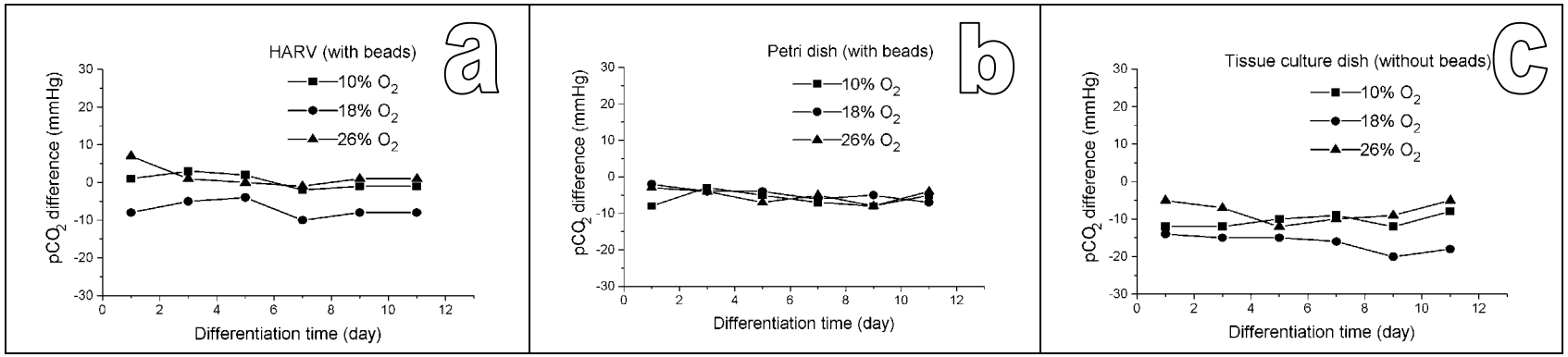

Figure 3.3d Comparison of pCO_2 differences in three culture vessels under culture conditions of hypoxia (10%), normoxia (18%) and hyperoxia (26%). pCO_2 differences were calculated by subtracting the steady state dissolved CO_2 (without cells) from the measured dissolved CO_2. Statistical comparison of pCO_2 differences (GLM procedure in SAS software package) of the plots returned the following results: a) 18% O_2 level vs 10% O_2 level (Pr =0.0001); 18% level O_2 vs 26% O_2 level (Pr =0.0001); b) 18% level O_2 vs 10% O_2 level (Pr =0.0695); 18% O_2 level vs 26% O_2 level (Pr =0.1691); c) 18% O_2 level vs 10% O_2 level (Pr =0.0021); 18% O_2 level vs 26% O_2 level (Pr =0.0373).

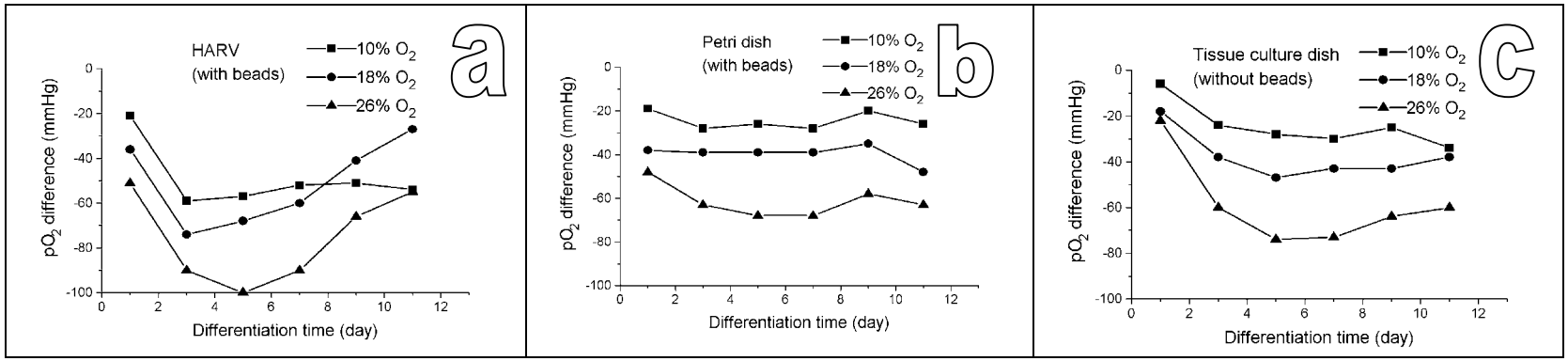

Figure 3.3e Comparison of pO_2 differences in three culture vessels under culture conditions of hypoxia (10%), normoxia (18%) and hyperoxia (26%). pO_2 differences were calculated by subtracting the steady state dissolved O_2 (without cells) from the measured dissolved O_2. Statistical comparison of pO_2 differences (GLM procedure in SAS software package) of the plots returned the following results: a) 18% O_2 level vs 10% O_2 level (Pr =0.1655); 18% O_2 level vs 26% O_2 level (Pr =0.0001); b) 18% O_2 level vs 10% O_2 level (Pr =0.0001); 18% O_2 level vs 26% O_2 level (Pr =0.0001); c) 18% O_2 level vs 10% O_2 level (Pr =0.0001); 18% O_2 level vs 26% O_2 level (Pr =0.0014).

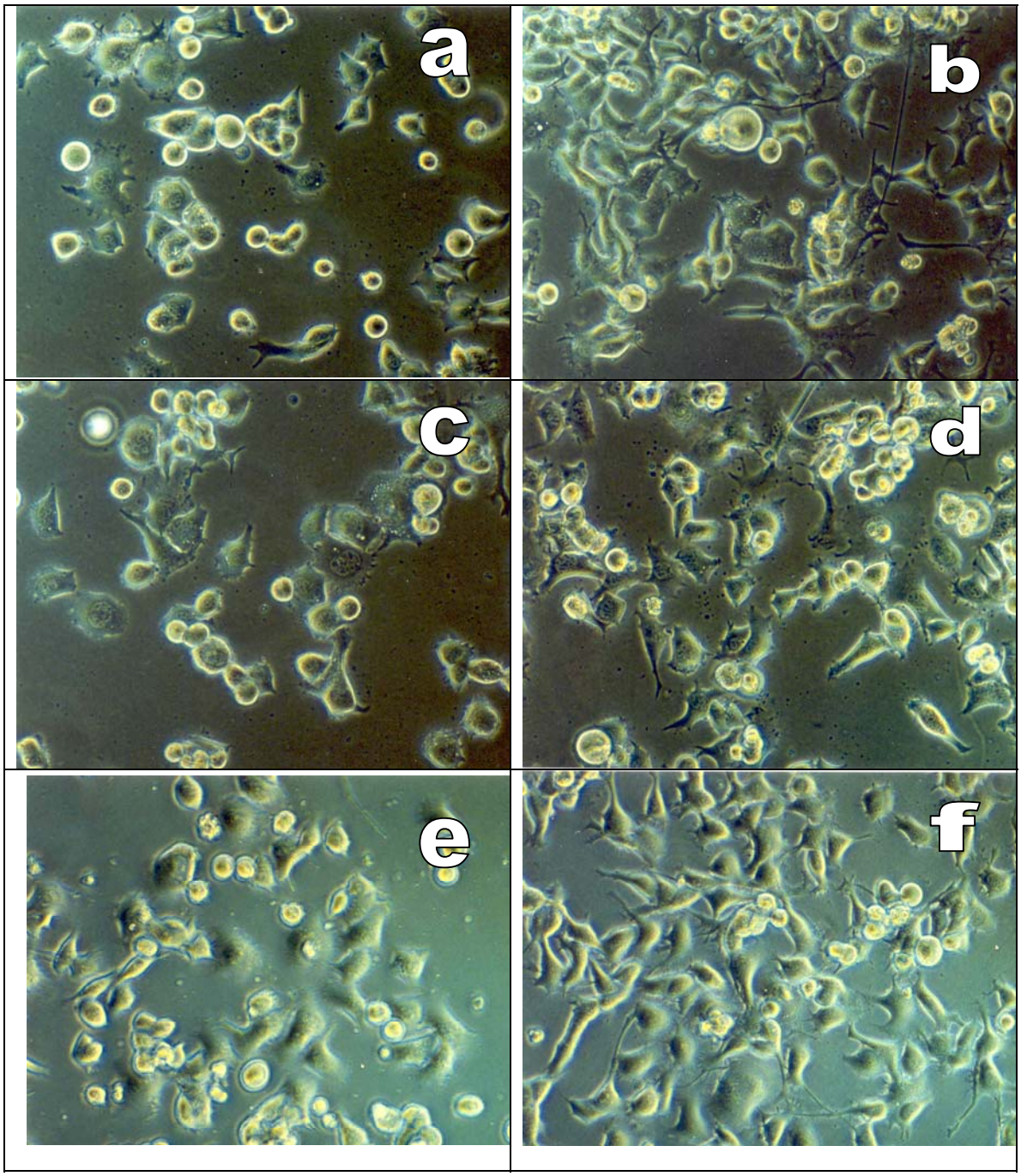

Figure 3.4 Comparison of N1E-115 cells differentiated in tissue culture dishes during the first two days. The first row shows the cells differentiated in 10% O_2 in the 1st (a) and 2nd (b) days; The second row shows the cells differentiated in 18% O_2 in the 1st (c) and 2nd (d) days; The third row shows the cells differentiated in 26% O_2 in the 1st (e) and 2nd (f) days;

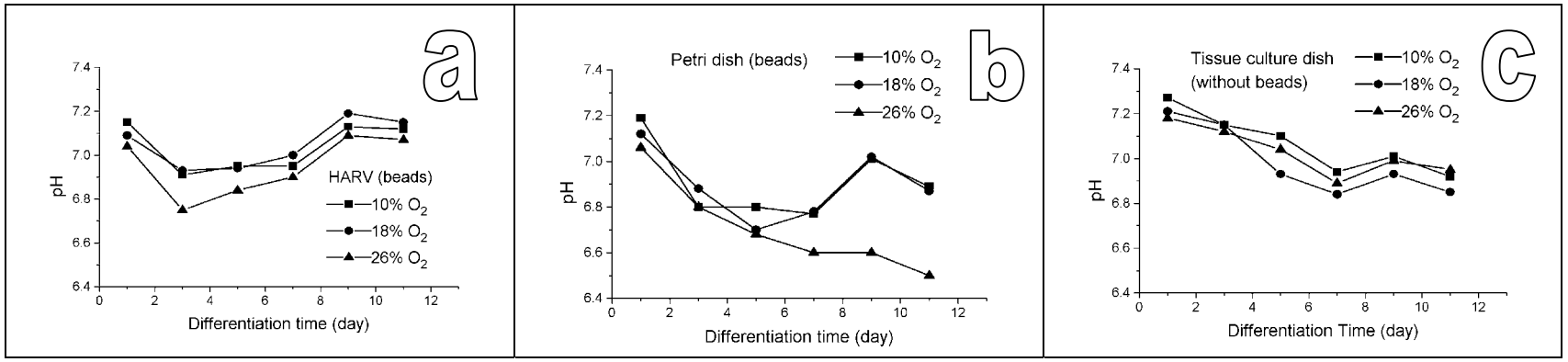

Figure 3.5 Comparison of pH in three culture vessels under culture conditions of hypoxia (10%), normoxia (18%) and hyperoxia (26%). Statistical comparison of pH (GLM procedure in SAS software package) of the plots returned the following results: a) 18% O_2 level vs 10% O_2 level (Pr =0.2170); 18% O_2 level vs 26% O_2 level (Pr =0.0041); b) 18% O_2 level vs 10% O_2 level (Pr =0.6162); 18% O_2 level vs 26% O_2 level (Pr =0.0001); c) 18% O_2 level vs 10% O_2 level (Pr =0.0124); 18% O_2 level vs 26% O_2 level (Pr =0.0494).

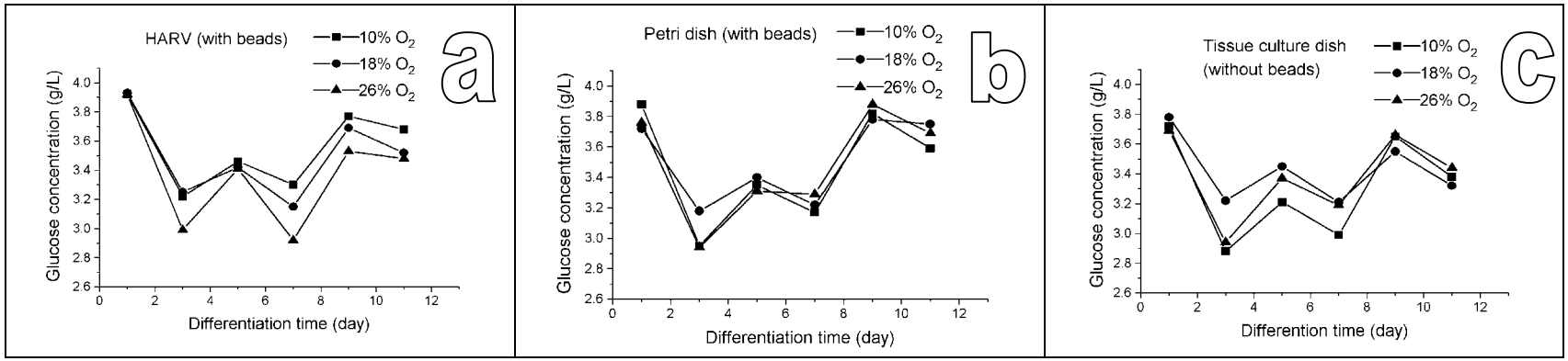

Figure 3.6 Comparison of glucose concentration in three culture vessels under culture conditions of hypoxia (10%), normoxia (18%) and hyperoxia (26%). Statistical comparison of glucose concentration (GLM procedure in SAS software package) of the plots returned the following results: a) 18% O_2 level vs 10% O_2 level (Pr =0.4617); 18% O_2 level vs 26% O_2 level (Pr =0.2699); b) 18% O_2 level vs 10% O_2 level (Pr =0.0918); 18% O_2 level vs 26% O_2 level (Pr =0.5027); c) 18% O_2 level vs 10% O_2 level (Pr =0.1556); 18% O_2 level vs 26% O_2 level (Pr =0.1600).

CHAPTER 4

CONCLUSIONS AND FUTURE DIRECTIONS

CONCLUSIONS

The results in this study support the following conclusions:

1) It was not possible to replicate color development by differentiating neuroblastoma cells under simulated microgravity suggesting that the phenomena previously observed in our laboratory and by other investigations was not solely dependent on microgravity, if at all.
2) Metabolic differences (O_2 consumption pattern) observed between cells differentiated under normal and microgravity were attributed more to O_2 mass transport limitation into the HARV.
3) Hopoxia was not proven to be a factor in transdifferentiation of N1E-115 neuroblastoma cells to melanocyte-like cells.

FUTURE DIRECTIONS

N1E-115 cells cultured in extremely low serum differentiation medium, in tissue culture dishes, exhibit morphological changes marked by the elaboration of an extensive network of neurite processes and decreased cell growth. These changes are accompanied by increases in the synthesis of neuron specific enzymes such as acetylcholinesterase,

neurotransmitters such as catecholamines, and the development of electrophysiological currents associated with in neural cells in vivo.

The studies conducted in this research did not address any of the above markers for differentiation, partly because neuron specific enzymes required a large amount of sample, which would not be raised in HARV after 10 days of differentiation.

One way to address this problem is to consider a molecular approach involving the use of gene analysis. Microgravity has been reported to alter protein phosphorylation-dependent cellular signaling, e.g. PKC activated pathway (de Groot et al., 1991). Some critical cellular signaling mechanisms involved in gene-regulation might be sensitive to the simulated microgravity environment. This approach does not require large amount of sample.

REFERENCES

1. de Groot, R. P.; P. J. Rijken; J. Den Hertog; J. Boonstra; A. J. Verkleij and W. Kruijer. Nuclear response to protein kinase C signal transduction are sensitive to gravity changes. *Exp. Cell Res*. **1991**, 197, 87-90.

APPENDIX A

RAW DATA FOR CHAPTER 3

Table A1.1 Metabolic activity results under the following N1E-115 cell growth/differentiation conditions:
Incubator oxygen level: 10%
Cell growth/differentiation vessel: HARV bioreactor
Cell anchorage substrate: Cytodex 3 beads

Differentiation Day	HARV Bioreactor	Parameters measured			
		pH	pCO_2 (mmHg)	pO_2(mmHg)	Glucose (g/L)
1	1A*	-	-	-	
	1B	-	-	-	4.20
	2A	-	-	-	
	2B	-	-	-	4.15
2	1A	7.10	74	74	
	1B	7.13	71	75	3.94
	2A	7.16	70	84	
	2B	7.18	70	83	3.90
4	1A	6.86	76	41	
	1B	6.89	71	51	3.11
	2A	6.79	74	35	
	2B	6.88	72	41	3.33
6	1A	6.91	71	43	
	1B	6.93	73	48	3.41
	2A	6.95	74	35	
	2B	6.99	71	49	3.51
8	1A	6.91	66	55	
	1B	6.87	68	45	3.28
	2A	7.05	70	57	
	2B	6.94	72	39	3.32
10	1A	7.10	71	42	
	1B	7.08	69	48	3.76
	2A	7.18	71	58	
	2B	7.15	67	51	3.78
12	1A	7.11	70	46	
	1B	7.09	70	46	3.66
	2A	7.10	71	48	
	2B	7.17	69	68	3.7

* A & B were parallel experiments; pH, pCO2 and pO2 were not measured since they did not reach stable state.

Table A1. 2 Metabolic activity results under the following N1E-115 cell growth/differentiation conditions:
Incubator oxygen level: 10%
Cell growth/differentiation vessel: tissue culture dish
Cell anchorage substrate: tissue culture dish bottom (vacuum gas plasma treated)

Differentiation day	Tissue culture dish	Parameters measured			
		pH	pCO_2 (mmHg)	pO_2(mmHg)	Glucose
1	1A*	-	-	-	
	1B	-	-	-	4.20
	2A	-	-	-	
	2B	-	-	-	4.15
2	1A	7.26	62	101	
	1B	7.25	63	100	3.75
	2A	7.27	58	109	
	2B	7.27	58	104	3.69
4	1A	7.16	65	83	
	1B	7.20	60	87	2.83
	2A	7.13	58	88	
	2B	7.11	60	84	2.93
6	1A	7.06	63	82	
	1B	7.13	64	83	3.16
	2A	7.10	63	78	
	2B	7.10	61	82	3.26
8	1A	6.88	66	79	
	1B	6.92	64	82	2.87
	2A	6.96	62	79	
	2B	7.01	61	79	3.11
10	1A	6.88	65	80	
	1B	7.01	61	89	3.67
	2A	7.03	58	82	
	2B	7.08	58	86	3.63
12	1A	6.79	67	75	
	1B	6.81	67	77	3.24
	2A	7.04	63	76	
	2B	7.03	63	75	3.52

* A & B were parallel experiments; pH, pCO2 and pO2 were not measured since they did not reach stable state.

Table A1.3 Metabolic activity results under the following N1E-115 cell growth/differentiation conditions:
Incubator oxygen level: 10%
Cell growth/differentiation vessel: petri dish
Cell anchorage substrate: Cytodex 3 beads

Differentiation Day	Petri-dish	Parameters measured			
		pH	pCO_2 (mmHg)	pO_2(mmHg)	Glucose
1	1A*	-	-	-	
	1B	-	-	-	4.20
	2A	-	-	-	
	2B	-	-	-	4.15
2	1A	7.14	66	85	
	1B	7.15	63	88	3.86
	2A	7.21	61	91	
	2B	7.22	61	94	3.90
4	1A	6.83	67	81	
	1B	6.86	69	80	2.89
	2A	6.75	65	83	
	2B	6.75	68	79	3.01
6	1A	6.80	66	77	
	1B	6.78	64	82	3.34
	2A	6.80	67	88	
	2B	6.82	66	81	3.36
8	1A	6.71	61	83	
	1B	6.69	60	86	3.05
	2A	6.88	66	72	
	2B	6.78	65	79	3.29
10	1A	6.85	65	87	
	1B	6.85	65	87	3.78
	2A	7.11	62	88	
	2B	7.23	59	91	3.74
12	1A	6.80	65	79	
	1B	6.85	65	79	3.67
	2A	6.87	67	87	
	2B	7.02	65	76	3.51

* A & B were parallel experiments; pH, pCO2 and pO2 were not measured since they did not reach stable state.

Table A2.1 Metabolic activity results under the following N1E-115 cell growth/differentiation conditions:
Incubator oxygen level: 18%
Cell growth/differentiation vessel: HARV bioreactor
Cell anchorage substrate: Cytodex 3 beads

Differentiation Day	HARV Reactor	Parameters measured			
		pH	pCO_2 (mmHg)	pO_2(mmHg)	Glucose (g/L)
1	1A*	-	-	-	
	1B	-	-	-	4.16
	2A	-	-	-	
	2B	-	-	-	4.16
2	1A	7.05	62	95	
	1B	7.06	64	97	3.90
	2A	7.12	57	96	
	2B	7.10	64	91	3.96
4	1A	6.91	65	61	
	1B	6.89	64	58	3.20
	2A	6.93	63	58	
	2B	6.96	64	52	3.3
6	1A	6.93	66	63	
	1B	6.93	65	63	3.33
	2A	6.94	64	62	
	2B	6.93	65	43	3.50
8	1A	6.99	57	68	
	1B	7.01	61	72	3.10
	2A	7.00	59	81	
	2B	6.98	62	62	3.21
10	1A	7.20	60	91	
	1B	7.16	60	92	3.59
	2A	7.20	63	91	
	2B	7.20	63	88	3.78
12	1A	7.09	61	107	
	1B	7.11	62	106	3.43
	2A	7.20	62	98	
	2B	7.20	60	104	3.60

* A & B were parallel experiments; pH, pCO2 and pO2 were not measured since they did not reach stable state.

Table A2.2 Metabolic activity results under the following N1E-115 cell growth/differentiation conditions:
Incubator oxygen level: 18%
Cell growth/differentiation vessel: tissue culture dish
Cell anchorage substrate: tissue culture dish bottom (vacuum gas plasma treated)

Differentiation day	Tissue culture dish	Parameters measured			
		pH	pCO_2 (mmHg)	pO_2(mmHg)	Glucose
1	1A*	-	-	-	
	1B	-	-	-	4.16
	2A	-	-	-	
	2B	-	-	-	4.16
2	1A	7.21	59	118	
	1B	7.17	60	118	3.81
	2A	7.22	61	119	
	2B	7.23	61	119	3.75
4	1A	7.12	60	97	
	1B	7.13	60	103	3.19
	2A	7.16	61	97	
	2B	7.15	59	98	3.25
6	1A	6.89	59	90	
	1B	6.91	58	92	3.55
	2A	6.93	63	85	
	2B	6.96	58	92	3.35
8	1A	6.83	57	92	
	1B	6.82	59	95	3.18
	2A	6.84	58	94	
	2B	6.86	58	92	3.24
10	1A	6.90	53	89	
	1B	6.96	57	91	3.44
	2A	6.94	54	96	
	2B	6.92	53	92	3.66
12	1A	6.80	56	99	
	1B	6.90	58	97	3.41
	2A	6.86	56	96	
	2B	6.84	55	103	3.23

* A & B were parallel experiments; pH, pCO2 and pO2 were not measured since they did not reach stable state.

Table A2.3 Metabolic activity results under the following N1E-115 cell growth/differentiation conditions:
Incubator oxygen level: 18%
Cell growth/differentiation vessel: petri dish
Cell anchorage substrate: Cytodex 3 beads

Differentiation Day	Petri-dish	Parameters measured			
		pH	pCO_2 (mmHg)	pO_2(mmHg)	Glucose
1	1A*	-	-	-	
	1B	-	-	-	4.16
	2A	-	-	-	
	2B	-	-	-	4.16
2	1A	7.15	62	103	
	1B	7.17	61	107	3.76
	2A	7.05	61	100	
	2B	7.09	59	100	3.68
4	1A	6.90	60	101	
	1B	6.91	58	102	3.16
	2A	6.83	58	97	
	2B	6.87	60	105	3.20
6	1A	6.66	60	98	
	1B	6.65	61	98	3.33
	2A	6.75	55	102	
	2B	6.73	58	107	3.47
8	1A	6.71	55	99	
	1B	6.77	59	101	3.19
	2A	6.60	56	105	
	2B	7.01	56	101	3.25
10	1A	7.01	59	104	
	1B	6.99	59	103	3.81
	2A	7.04	56	106	
	2B	7.04	56	107	3.75
12	1A	6.90	56	96	
	1B	6.96	57	94	3.77
	2A	6.90	52	108	
	2B	6.68	57	112	3.73

* A & B were parallel experiments; pH, pCO2 and pO2 were not measured since they did not reach stable state.

Table A3.1 Metabolic activity results under the following N1E-115 cell growth/differentiation conditions:
Incubator oxygen level: 26%
Cell growth/differentiation vessel: HARV bioreactor
Cell anchorage substrate: Cytodex 3 beads

Differentiation Day	HARV Reactor	Parameters measured			
		pH	pCO_2 (mmHg)	pO_2(mmHg)	Glucose (g/L)
1	1A*	-	-	-	
	1B	-	-	-	4.18
	2A	-	-	-	
	2B	-	-	-	4.15
	3A	-	-	-	
	3B	-	-	-	4.15
2	1A	7.03	76	117	
	1B	7.01	75	120	3.87
	2A	7.04	74	123	
	2B	7.06	76	127	3.95
	3A	7.12	82	140	
	3B	7.14	81	145	3.91
4	1A	6.70	69	85	
	1B	6.74	68	79	2.96
	2A	6.74	72	83	
	2B	6.82	70	84	3.01
	3A	6.97	85	102	
	3B	6.95	84	114	2.93
6	1A	6.76	71	68	
	1B	6.82	68	72	3.36
	2A	6.88	69	76	
	2B	6.89	66	75	3.46
	3A	6.94	86	118	
	3B	6.91	83	125	3.33
8	1A	6.83	68	84	
	1B	6.84	68	85	2.88
	2A	6.94	67	82	
	2B	6.98	66	78	2.95
	3A	7.14	81	138	
	3B	7.10	82	142	2.84
10	1A	7.10	72	103	
	1B	7.02	69	117	3.46
	2A	7.10	69	101	
	2B	7.11	67	105	3.60
	3A	7.09	79	154	
	3B	7.12	81	152	3.45
12	1A	7.01	68	131	
	1B	7.08	70	109	3.43
	2A	7.09	68	111	
	2B	7.08	71	118	3.52
	3A	7.15	81	147	
	3B	7.16	79	156	3.42

* A & B were parallel experiments; pH, pCO2 and pO2 were not measured since they did not reach stable state.

Table A3.2 Metabolic activity results under the following N1E-115 cell growth/differentiation conditions:
Incubator oxygen level: 26%
Cell growth/differentiation vessel: tissue culture dish
Cell anchorage substrate: tissue culture dish bottom (vacuum gas plasma treated)

Differentiation day	Tissue culture dish	Parameters measured			
		pH	pCO_2 (mmHg)	pO_2(mmHg)	Glucose
1	1A*	-	-	-	
	1B	-	-	-	4.18
	2A	-	-	-	
	2B	-	-	-	4.15
	3A	-	-	-	
	3B	-	-	-	4.15
2	1A	7.19	68	158	
	1B	7.17	67	152	3.58
	2A	7.18	65	160	
	2B	7.18	65	159	3.80
	3A	7.22	73	142	
	3B	7.22	72	172	3.82
4	1A	7.11	64	118	
	1B	7.09	65	119	2.89
	2A	7.12	62	111	
	2B	7.15	66	126	2.99
	3A	7.13	81	146	
	3B	7.14	77	146	2.91
6	1A	7.01	61	109	
	1B	7.02	61	104	3.45
	2A	7.05	58	108	
	2B	7.05	60	101	3.29
	3A	7.07	71	142	
	3B	7.03	75	147	3.34
8	1A	6.88	62	104	
	1B	6.88	64	108	3.26
	2A	6.85	63	102	
	2B	6.95	57	113	3.12
	3A	7.02	78	141	
	3B	7.14	75	141	3.18
10	1A	6.94	64	122	
	1B	7.00	63	106	3.53
	2A	7.00	61	116	
	2B	7.02	63	114	3.79
	3A	7.09	80	151	
	3B	7.12	75	157	3.70
12	1A	6.86	8	19	
	1B	6.82	64	12	3.49
	2A	6.96	65	120	
	2B	6.94	66	118	3.39
	3A	7.18	77	152	
	3B	7.18	76	156	3.40

* A & B were parallel experiments; pH, pCO2 and pO2 were not measured since they did not reach stable state.

Table A3.3 Metabolic activity results under the following N1E-115 cell growth/differentiation conditions:
Incubator oxygen level: 26%
Cell growth/differentiation vessel: petri dish
Cell anchorage substrate: Cytodex 3 beads

Differentiation Day	Petri-dish	Parameters measured			
		PH	pCO_2 (mmHg)	pO_2(mmHg)	Glucose
1	1A*	-	-	-	
	1B	-	-	-	4.18
	2A	-	-	-	
	2B	-	-	-	4.15
	3A	-	-	-	
	3B	-	-	-	4.15
2	1A	7.07	66	130	
	1B	7.06	66	130	3.80
	2A	7.05	64	143	
	2B	7.05	65	140	3.72
	3A	7.14	79	149	
	3B	7.14	77	147	3.82
4	1A	6.71	63	100	
	1B	6.71	62	103	3.00
	2A	6.88	67	123	
	2B	6.87	65	123	2.88
	3A	7.07	71	123	
	3B	7.04	74	110	2.95
6	1A	6.62	59	119	
	1B	6.60	62	114	3.36
	2A	6.71	63	114	
	2B	6.77	61	116	3.26
	3A	6.87	79	126	
	3B	6.93	76	141	3.33
8	1A	6.54	63	116	
	1B	6.60	63	110	3.27
	2A	6.62	66	116	
	2B	6.62	64	120	3.31
	3A	7.17	74	142	
	3B	7.18	70	146	3.26
10	1A	6.65	62	121	
	1B	6.69	61	134	3.91
	2A	6.51	60	121	
	2B	6.52	60	125	3.85
	3A	7.15	72	149	
	3B	7.12	70	158	3.80
12	1A	6.71	62	131	
	1B	6.73	60	133	3.75
	2A	6.44	62	120	
	2B	6.53	63	121	3.63
	3A	7.18	76	153	
	3B	7.11	75	153	3.77

* A & B were parallel experiments; pH, pCO2 and pO2 were not measured since they did not reach stable state.

Table A4.1 pH of differentiation medium in culture vessels without cells

Oxygen Level	HARV			Petri-dish			Tissue culture dish		
	1	2	average	1	2	Average	1	2	average
10%	7.25	7.25	7.25	7.23	7.24	7.24	7.24	7.23	7.24
18%	7.25	7.24	7.25	7.30	7.30	7.30	7.23	7.24	7.24
26%	7.22	7.23	7.23	7.28	7.29	7.29	7.18	7.19	7.19

Table A4.2 Dissolved pCO_2 of differentiation medium in culture vessels without cells

Oxygen Level	HARV (mmHg)			Petri-dish (mmHg)			Tissue culture dish (mmHg)		
	1	2	average	1	2	Average	1	2	average
10%	71	71	71	72	71	71	73	74	73
18%	69	70	70	62	63	63	76	74	75
26%	69	69	69	68	70	69	71	72	72

Table A4.3 Dissolved pO_2 of differentiation medium in culture vessels without cells

Oxygen Level	HARV (mmHg)			Petri-dish (mmHg)			Tissue culture dish (mmHg)		
	1	2	average	1	2	Average	1	2	average
10%	101	100	101	109	108	109	109	110	110
18%	130	131	131	141	140	141	136	137	137
26%	174	172	173	182	185	184	180	179	180

Table A5.1 Protein analysis results before differentiation

Culture vessel	HARV	Petri dish	Tissue culture dish
Working volume	50 ml	15 ml	15 ml
Cell inoculation (cells/cm^2)	8889 (on bead)	8889 (on bead)	8889 (on bottom surface)
Inoculation protein ($\mu g/cm^2$)	11.4	11.4	11.4

Table A5.2 Protein analysis results after 12 days of culture in differentiation medium

Culture vessel	Protein ($\mu g/cm^2$)					
	Hypoxia (10% O_2)		Normoxia (18% O_2)		Hyperoxia (26% O_2)	
HARV	A*	2.30	A	3.44	A	2.91
	B	1.92	B	3.07	B	2.92
Petri dish	A	4.26	A	4.98	A	5.34
	B	4.55	B	6.70	B	5.03
Tissue culture dish	A	5.05	A	7.52	A	5.88
	B	5.70	B	6.85	B	6.60

* A & B were parallel experiments.

Table A5.3 Cell viability after 12 days of culture in differentiation medium

Culture vessel	Cell viability					
	Hypoxia (10% O_2)		Normoxia (18% O_2)		Hyperoxia (26% O_2)	
HARV	A*	20.2%	A	30.2%	A	25.5%
	B	16.8%	B	26.9%	B	25.6%
Petri dish	A	37.4%	A	43.7%	A	46.8%
	B	39.9%	B	58.8%	B	44.1%
Tissue culture dish	A	44.3%	A	66.0%	A	51.6%
	B	50.0%	B	60.1%	B	57.9%

* A & B were parallel experiments.

Table A6.1 Tyrosinase activity analysis results before and after 12 days of culture in differentiation medium

Culture vessel	Tyrosinase activity (unit)						
	Before differentiation (cells without beads)	After 12 days of culture in differentiation medium					
		Hypoxia (10% O_2)		Normoxia (18% O_2)		Hyperoxia (26% O_2)	
HARV	0	A*	9.59	A	15.00	A	12.47
	0	B	7.95	B	12.60	B	10.69
Petri dish	0	A	5.69	A	8.22	A	12.54
	0	B	4.38	B	10.07	B	11.37
Tissue culture dish	0	A	0	A	0	A	0
	0	B	0	B	0	B	0

* A & B were parallel experiments.

APPENDIX B

LABORATORY PROTOCOLS

B1 MEDIUM PREPARATION

Reagents:

1. GIBCO: DMEM (Dulbelcco's Modified Eagle medium)-Cat. # 12100-103;
2. GIBCO: Pen-Strep (Penicillin-Streptomycin)-Cat. # SV30010;
3. HYCLONE: FBS (Fetal Bovine Serum)-Cat. # SH30071.03;
4. SIGMA: DMSO-Cat.# D2650

Full DMEM stock (for example, 2L)

Measure out 1900 ml of deionized H_2O into a 4 L flask, add 26.76 g DMEM powder medium at room temperature. Stir slowly, add 7.4 g $NaHCO_3$, adjust the pH to 6.7~6.8 using 1 N HCl. Add remaining deionized H_2O and make up volume to 2 L, sterilize immediately by membrane filtration. Store at 4 ^{0}C until need.

Growth medium (86%DMEM+13%FBS+1%Pen-Strep, for example, 1 litter)

Full DMEM: 860ml

FBS: 130ml

Pen-Strep: 10ml

Differentiating medium (98.5%DMEM+0.5%FBS+1%Pen-Strep, for example, 1 litter)

Full DMEM: 860ml

FBS: 5ml

Pen-Strep: 10ml

Procedures for making growth medium and differentiation medium

1. Obtain full DMEM stock from the fridge (1L)
2. Add 10 ml Pen-Strep
3. Divide into 500 ml fractions
4. Add 65ml FBS to each 500 ml fraction to obtain the tissue culture medium
5. Add 2.5ml FBS to each 500 ml fraction to obtain the differentiating medium.

B2 STERILIZATION OF HARV MICROGRAVITY BIOREACTOR

Non autoclave method: Completely fill the vessel with absolute alcohol and soak overnight. Thoroughly rinse the vessel with sterile phosphate buffered solution at least 3 times to remove traces of alcohol. Fill the vessel with the medium of choice and then leave it overnight.

B3 BEAD PREPARATION FOR HARV

Procedures:

1. Add 40ml Calcium/Magnesium Free (CMF) PBS into a 50ml centrifuge tube.
2. Weigh out 0.8g dry Cytodex® 3 beads.
3. Suspend the beads for swelling in the tube, place it at room temperature for 3 hours.
4. Aspirate the supernatant buffer.
5. Wash the beads by adding fresh CMF-PBS.
6. Let beads settle out and then aspirate.
7. Repeat the above 5 & 6 washing steps at least twice.
8. Resuspend the beads in fresh CMF-PBS, sterilize by autoclaving (115^0C, 15 min, 15 psi), cytodex is extremely stable and can be autoclaved repeatedly at least 5 cycles or extensively (130^0C, 12h, 27 psi) without affecting the performance. Or resuspend the beads in 70% ethanol, keep them at room temperature overnight, and then wash the beads 3 times with sterile CMF-PBS.
9. Rinse the beads with sterile culture medium, Resuspend in 40ml fresh culture medium.

B4 HARV BIOREACTOR CONDITIONING

Procedure:

1. If the center bolt has been loosened; in a sterile environment, gently tighten the center bolt with allen wrench. Note: do not over tighten, as this will strip the treads on the oxygenator core.
2. Fill the vessel with the medium of choice.
3. Wipe ports with sterile alcohol pad and attach sterile ¼ inch fill port cap.
4. Close syringe port valves.
5. Fill a 20 ml sterile syringe with the medium of choice, wipe one syringe with an alcohol pad and attach syringe.
6. Wipe the other syringe port with an alcohol pad and attach an empty 5- or 10- ml sterile syringe.
7. Gently invert vessel and tap on sides to expel air bubbles from under the ports. Maneuver air bubbles under the empty syringe. With both valves open, gently press on the syringes to replace air bubbles with medium.
8. When all bubbles are removed, close the syringe valves and discard the small syringe. Wipe the port with an alcohol pad and replace the cap.
9. Leave the large medium filled syringe on the unit with the valve open, as the volume of the medium in the vessel will expand slightly as it warms to 37 ^{o}C.
10. Attach the vessel to the rotator base and place them in a humidified CO_2 incubator.
11. Attach the power cord to the rotator base and pass the flat cable through the incubator door seal. Attach the other end of the flat cable power cord to the power supply. Note: the power supply is always located outside of the incubator.

12. Insure the rotator base is level.
13. Set the initial rotation speed to 12-14 rpm.
14. Rotate the vessel overnight, check for leaks and sterility.

B5 CALCULATION FOR THE NUMBER OF BEADS AND INOCULATING CELLS NEEDED IN HARV BIOREACTOR

Procedure:

1. 0.8 g beads reconstituted to a 40ml volume of medium will give a bead suspension concentration of 20mg/ml (based on dry weight).
2. The concentration usually used in the bioreactor is 5mg/ml (based on dry weight). So, we need to dilute the bead with cell suspension by the ratio of 1:4 (1ml bead suspension + 3ml cell suspension).
3. The specification sheet indicated there is approximately 3.0×10^6 beads/g dry weight, the surface area is 2,700 cm^2/g dry weight. So after dilution, bead suspension concentration: 5mg/ml × 3000 beads/mg = 15,000 beads/ml
4. Total beads in the 50 ml bioreactor: 15,000 beads/ml × 50ml=7.5×10^5 beads.
5. Total surface area of the beads in the 50 ml bioreactor: 675 cm^2.
6. Inoculate cells at 6 cells/bead, then in the 50 ml bioreactor,

   If required 6 cells/bead, the total cell number we need:

   6 cells/bead × 7.5×10^5 beads = 4.5 million cells

   Total cells/total surface=$4.5\times10^6/675cm^2$ =6.67×10^7 cells/m^2

   If required 7 cells/bead, the total cell number we need:

7 cells/bead × 7.5×10^5 beads = 5.25 million cells

Total cells/total surface=$5.25\times10^6/675cm^2$ =7.78×10^7 cells/m^2

If required 8 cells/bead, the total cell number we need:

8 cells/bead × 7.5×10^5 beads = 6 million cells

Total cells/total surface=$6.0\times10^6/675cm^2$ =8.89×10^7 cells/m^2

7. In the 50 ml bioreactor, we need:

Volume of bead suspension: V_1=12.5 ml (7.5×10^5 beads, 675 cm^2 bead surface)

Volume of cell suspension: V_2 = Total cells/cell suspension concentration (ml)

Volume of medium to be added for the full 50 ml: V_3=50-12.5-V_2 (ml)

B6 HARV INNOCULATION

Procedure:

1. Take out flasks from incubator, aspirate 20 ml suspension from each flask.
2. Use cell scraper thoroughly scrape cells from the wall of T-flask.
3. Flame pipet tip, use it transfer the suspension to a 15 ml centrifuge.
4. Centrifuge for 10 min at 500g and 4 ^{0}C, aspirate supernatant, squirt into beaker.
5. Add 5 ml new medium to each centrifuge tube.
6. Resuspend the pellet in DMEM growth medium using a Pasteur pipet, make sure mix thoroughly.
7. Aspirate 100 μl suspension and 100 μl Trypan Blue separately, put them into a micro-centrifuge tube, mix thoroughly, take 20 μl solution for Cell counting.
8. Fill the bioreactor to 50% of total volume with growth medium, allowing space to load cells and microcarrier beads, and then transfer the calculated amount of cell suspension into bioreactor.

B7 PROTIEN MICROASSAY PROCEDURE FOR MICROTITER PLATES

Materials:

1. Bio-Rad Detergent compatible (DC) Protein Assay Kit II (reagent A, S, and B).
2. Triton-100.
3. Detergent buffer: Add 0.25ml Triton-100 (0.5%, v/v) to 50ml 20 mM potassium phosphate (pH7.5).
4. Detergent and inhibitor buffer: Add 200µl protease inhibitor cock tail (P8340, Sigma) to 2 ml detergent buffer when to make standard curve.
5. 96 well Microtiter Plate.
6. Microplate Mixer.
7. Microplate Reader equipped with a band filter 750 nm.

Procedure:

1. Add 20ml dH_2O to Bovine Serum Albumin (BSA) standard (from kit) to yield solution of 1.43mg/ml. Mix thoroughly. Aliquot in 1ml portions to be stored at –20˚C.
2. Add 1ml BSA stock (1.43mg/ml) to 4ml dH_2O in a 15ml centrifuge tube. Label as "286µg/ml BSA solution."
3. Preparation of working reagent:

Add 20 µl of reagent S to each ml of reagent A that will be needed for the run. (This working reagent A' is stable for 1 week even though a precipitate will form after 1 day. If precipitate forms, warm the solution and vortex. Do not pipet the undissolved precipitate, as this will likely plug the tip of the pipet, thereby altering the volume of reagent that is

added to the sample). If samples do not contain detergent, you may omit this step and simply use reagent A as supplied.

4. Perform calculations to get appropriate range of standards. Use 286µg/ml BSA stock.

   Standard 1: (286µg/ml)(10µl)/(120µl) = 23.8 µg/ml

   Standard 2: (286µg/ml)(30µl)/(120µl) = 71.5 µg/ml

   Standard 3: (286µg/ml)(50µl)/(120µl) = 119.2 µg/ml

   Standard 4: (286µg/ml)(70µl)/(120µl) = 166.8 µg/ml

   Standard 5: (286µg/ml)(90µl)/(120µl) = 214.5 µg/ml

5. Prepare 120 µl of standards and samples in the appropriate clean, dry test tubes according to the following table.

Table B7.1 Standard curve BSA (linear range: 7.0 µg/ml - 65 µg/ml)

	Blank	Standard 1	Standard 2	Standard 3	Standard 4	Standard 5
Stock BSA (286µg/ml)	0	10 µl	30 µl	50 µl	70 µl	90 µl
DI water	90 µl	80 µl	60 µl	40 µl	20 µl	0 µl
Detergent and Inhibitor buffer	30 µl	30 µl	30 µl	30 µl	30 µl	30 µl
Final BSA Concentration (µg/ml)	0	23.8	71.5	119.2	166.8	214.5
Sample						
DI water			90 µl			
Extracted sample volume			30 µl			

6. Add 100 µl reagent A' or A (see note form step 3) into each test tube and vortex.
7. Add 800 µl reagent B into each tube and vortex immediately.
8. After 15 minutes, absorbances can be measured at 750 nm. Standards should be assayed in triplicate. Samples will be assayed in duplicate. Absorbance values will be stable for at least one hour.
9. Calculation:

   protein (µg) = calculated concentration (µg/1000µl) x 120 (µl) x 2000 (µl) / 30 (µl)

Protein sample preparation:

1. Centrifuge cells and/or beads at 500g for 10 min and remove the supernatant.
2. Re-suspend cells by vortexing in 2ml detergent buffer and 200 µl proteinase inhibitor cocktail for 5 min. Centrifuge the extracts at 9000g and 4 ^{0}C for 15 min, repeat centrifugation once.
3. Freeze the supernatant at -20 ^{0}C for future analysis.

B8 STANDARD STOPPED MBTH TYROSINASE ASSAY

Materials:

1. Detergent buffer (50ml)

   50ml 20 mM potassium phosphate (pH7.5);

   0.25ml Triton-100 (0.5%, v/v);

   protease inhibitor cocktail 5ml.

2. Assay buffer:

   100 mM potassium phosphate (pH7.1)

   4% (v/v) N, N'-dimethylformamide (liquid)

   0.1% (v/v) Triton X-100 (liquid)

3. 5 mM L-dopa
4. 25 mM hydrazone 3-methyl-2-benzothiazoninone hydrazone (MBTH)
5. 1 M perchloric acid
6. Standard tyrosinase (50 mg, MW ~125000, activity > 2000 U/mg, Fluka)
7. Dialysis membrane
8. 1.5 ml eppendorf tube
9. 96 wells MICROTEST tissue culture plate

Equipment:

1. Microcentrifuge (9000g)
2. Spectrophotometer (490nm)
3. MRX Microplate Reader, DYNEX Technologies, Inc.
4. Branson 1200 Sonicate machine (setting 5 μm)

Optimized enzyme preparation:

1. Re-suspend cells by vortexing in 2 ml detergent buffer and 200 µl proteinase inhibitor cocktail for 5 min.
2. Sonicate the above mixture in ice water for 30 s (setting 5 µm).
3. Centrifuge the extracts at 9000g and 4 ^{0}C for 15 min, repeat centrifugation once.
4. Dialyze the final supernatant against 20 mM potassium phosphate (pH7.5) (1 liter for 1 h, then 4 liter overnight).
5. Freeze at -20 ^{0}C for future analysis.

Procedures:

1. Prepare 2 reaction mixtures (A and B) without enzyme in 1.5 ml eppendorf tube, the reaction mixture is 0.47 ml, which contains:

    250 µl of assay buffer

        100 mM potassium phosphate (pH7.1);

        4% (v/v) N, N'-dimethylformamide;

        0.1% (v/v) Triton X-100.

    100 µl of 5 mM L-dopa

    120 µl of 25 mM MBTH

2. Add 140 µl of enzyme extract to B as sample, 126 µl of detergent buffer and 14 µl protease inhibitor cock tail to A as blank. This makes the total reaction mixture volume reach 610 µl, see the table below.
3. Add 1ml tyrosinase stock (0.25mg/ml) to 24ml detergent buffer in a 40ml centrifuge tube. Label as "10µg/ml tyrosinase standard solution."

4. Perform calculations to get appropriate range of standards. Use 10µg/ml standard stock.

Table B8.1 Standard tyrosinase curve (0.0~0.33 µg/ml)

Position	Reaction mixture	Standard Enzyme (10µg/ml)	Detergent buffer	Protease inhibitor cock tail	Total Volume	final Enzyme Conc.	Average OD reading
	(µl)	(µl)	(µl)	(µl)	(µl)	(µg/ml)	
Blank	470	0	126	14	610	0.0	
S1	470	4	122	14	610	0.07	
S2	470	8	118	14	610	0.13	
S3	470	12	114	14	610	0.20	
S4	470	16	110	14	610	0.26	
S5	470	20	106	14	610	0.33	
		Enzyme extract (µl)					
Sample	470	140	0	0	610		

Table B8.2 Standard tyrosinase curve (0.0~2.0 µg/ml)

Position	Reaction mixture	Standard Enzyme (10µg/ml)	Detergent buffer	Protease inhibitor cock tail	Total Volume	final Enzyme Conc.	Average OD reading
	(µl)	(µl)	(µl)	(µl)	(µl)	(µg/ml)	
Blank	470	0	126	14	610	0.0	
S1	470	12	114	14	610	0.20	
S2	470	30	96	14	610	0.49	
S3	470	60	66	14	610	0.98	
S4	470	90	36	14	610	1.48	
S5	470	120	6	14	610	1.97	
		Enzyme extract (µl)					
Sample	470	140	0	0	610		

* There is 14 µl protease inhibitor cocktail in the 140 µl sample

5. Incubate the mixture at 37 ^{0}C water bath for 10 min.

6. Stop the reaction by adding 500 µl of 1 M perchloric acid.

7. Microcentrifuge (9000g for 5 min) the mixture at room temperature.
8. Transfer 350 µl of supernatant directly to a 96 well microtiter plate.
9. Measure the absorbance at 490nm using a spectrophotometer.
10. Calculate tyrosinase content by the standard tyrosinase response curve.

Reference:

[1] Alison J Winder, (1994), J. Biochem. Biophys. Methods 28: 173-183.

[2] Alison J Winder and Henry Harris, (1991), Eur. J. Biochem. 198, 317-326.

B9 GLUCOSE ANALYSIS BY SHIMADZU HPLC

Standard materials: Glucose

Column: Corgel 64H (Transgenomic, L=300nm, ID=7.8mm)

Eluant: 4 mN H_2SO_4

Flow Rate: 0.6 ml/min

Oven temp: 60^oC

Method: Orgacid2.mth

Run time: 30 min

Start-up

1. Prepare eluant: eluant for glucose analysis is 4mN H_2SO_4. Vacuum filter through 0.45 μm filter. After filtration, tilt the reservoir and pour eluant down the side of the reservoir slowly, avoiding making air bubbles. Rinse glassware by deionized water. When returning eluant to pump, make sure that the intake pipe to the pump has eluant in it, not air. If there is any air in the pipe, the pump will not properly work and could be damaged. Air may get in the column and cause a bad base line. Putting the intake pipes in another bottle of eluant or beaker of water while filtering the eluant will help reduce this problem.
2. Start Helium sparging by opening tank and setting regulator to 6 psi, barely on. Bubbling should be slow.
3. Flow eluant through pump, column and detector at 0.4 mL/min for 30 min with oven off. Adjust flow rate by software using icon with yellow box, then choosing parameters from subsequent menu, typing the correct flow in T Flow square and pressing Download button. Pump is on if the green light by the word pump is lit. If

not, depress the square button on right face to turn pump on. If the pump gauge indicates that there is no pressure, air is in the pump and it needs to be purged. To purge the pump, open the dial on the right side of the pump to divert the flow away from the column. There is a waste pipe existing at the bottom of the dial. Disconnect it at the tee beside the oven and connect a syringe to the end of the pipe. Start pumping and pull eluant through the pump until it drips regularly from the pipe without syringe. If the pump intake pipe is completely empty of eluant, first unscrew it from the bottom of the pump head, fill it with eluant and replace it. Be careful no to screw it too tightly.

4. Turn column oven on by pressing the square button on oven and flow for 20 minutes. Oven temperature should be set at 60^{o}C manually on oven face.
5. Increase flow to 0.6 mL/min. To purge, press second function purge/9 on the RI face; To end purge, press second function purge/9 again. Purge RI for 20 minutes.
6. Check for a flat baseline for 30 minutes by choosing the icon preview and pressing second function, auto zero/6 on the RI face. Choose the stop icon to stop the baseline preview.
7. Fill out logbook, including the pump pressure, which can be found on the Shimadzu controller above the oven. Press the button "Monitor" to display current conditions. Pressure is found beside the label A, and should be 50~55 kgf/cm^2 at a flow rate of 0.6 mL/min and oven temperature at 60^{o}C.

Run Samples:

Filter samples through 0.45 μm syringe filters into 1.5 ml vials and cap with white teflon septa, label vials with owner's initials and reference number. Don't use tape; Set

up a Batch file; Choose the icon Run Batch to begin injections. If injecting only one sample, still use Run Batch and set it to inject two samples; Analyze data by opening each data file using the green data icon and choosing icon Analyze. If the HPLC will not be used for 24 hours, shut it down.

Shut Down:

Remove all vials from rack. Autoclave if they contain bacteria, save and wash yellow caps; Turn the column oven off and flow at 0.4 mL/min for 30 minutes; Stop flow and turn off Helium.

B10 pH, pCO_2, pO_2 ANALYSIS BY RADIOMETER ABL5

Operation conditions:

Temperature: 15 ~32^{o}C;

Sample volume: 35 µl;

Sample handling time: 60 sec;

Measurement mode: blood (default);

Sample introduction: aspirate from sample inlet.

Installation and setup programs (first time use):

Condition and membrane electrodes, mount electrodes to the machine. Setup and startup the analyzer. Set up the following programs: Radiometer setup; Calibration setup; Barometer adjustment; Derived parameters; Units; Time/date; Auto Print/send; Interface setup; Gas percentages; Analyzer ID.

Start up:

Start up lasts approximately 20 minutes in order to warm up the electrode, including the programs of power on, LS adjustment, refill and start up calibration (Cal 2).

Run samples:

Check solutions, if insufficient, replace them using new solution. Activate ABL5 from standby state. Using syringe take 3~4 ml media sample from bioreactors for an immediate analysis. Slant the sample aspiration inlet, insert the inlet into the syringe well below the surface, press the aspirate button to aspirate samples, once a beep is heard, the aspiration is done, push the inlet to its original position. The ABL5 will automatically start to analyze the sample and print out analytical results after a couple of minutes.

Maintenance:

1. After an analysis, Radiometer will automatically perform the rinse program.
2. If there is a need to remove lipid or protein deposits from the measuring system, the cleaning program or protein removal program should be used. Otherwise, cleaning program should be performed once a day, and protein removal program should be performed once a week or after 100 samples.
3. Hold analyzer program: always perform the following procedures in the Hold Mode, remembraning the electrode (once a month for pO_2, pCO_2 and reference electrode); replace the electrode; replace the solutions; replace the pump tubing; replace the premixed gas cylinders; cleaning the inlet; replace the waste container; cleaning the measuring chamber.
4. Refill program: fill liquid transport system with the solutions and to flush gas lines.
5. LS adjustment program: adjusts the liquid sensor in the wet section of the ABL5.

Shut down:

Press menu to enter utilities, press standby to enter Standby Mode, this is a temporary shut down of the analyzer in order to keep the electrodes conditioned and the temperature in the thermostatted unit at $37.0 \pm 0.2\ ^{o}C$. Hit start button to activate ABL5 from Standby Mode for analysis.

APPENDIX C

SAS PROGRAM FOR ANALYSIS OF VARIANCE

USING THE GENERAL LINEAR MODEL (GLM)

GLM models used in the following SAS programs:

1) Model used to compare the curves in Figure 3.3a_a

$$pO_2 = \alpha_{reactor} + \beta_{time} + replicat(reactor) + \alpha_{reactor}*\beta_{time} + \varepsilon$$

2) Model used to compare the curves in Figure 3.3a_b, 3.3b

$$pO_2\_difference = \alpha_{reactor} + \beta_{time} + replicat(reactor) + \alpha_{reactor}*\beta_{time} + \varepsilon$$

3) Model used to compare the curves in Figure 3.3a_c

$$pCO_2 = \alpha_{reactor} + \beta_{time} + replicat(reactor) + \alpha_{reactor}*\beta_{time} + \varepsilon$$

4) Model used to compare the curves in Figure 3.3a_d, 3.3c

$$pCO_2\_difference = \alpha_{reactor} + \beta_{time} + replicat(reactor) + \alpha_{reactor}*\beta_{time} + \varepsilon$$

5) Model used to compare the curves in Figure 3.3d

$$pCO_2\_difference = \alpha_{oxygen\_level} + \beta_{time} + replicat(oxygen\_level) + \alpha_{oxygen\_level}*\beta_{time} + \varepsilon$$

6) Model used to compare the curves in Figure 3.3e

$$pO_2\_difference = \alpha_{oxygen\_level} + \beta_{time} + replicat(oxygen\_level) + \alpha_{oxygen\_level}*\beta_{time} + \varepsilon$$

7) Model used to compare the curves in Figure 3.5

$$pH = \alpha_{oxygen\_level} + \beta_{time} + replicat(oxygen\_level) + \alpha_{oxygen\_level}*\beta_{time} + \varepsilon$$

8) Model used to compare the curves in Figure 3.6

$$glucose = \alpha_{oxygen\_level} + \beta_{time} + replicat(oxygen\_level) + \alpha_{oxygen\_level}*\beta_{time} + \varepsilon$$

//sas program used to compare the curves in Figure 3.3a_a

```
options ls=78 nodate;
data one;
        infile 'c:\weicheng\7.prn';
        input reactor $ time replicat pO2;
proc glm data=one;
        class reactor time replicat;
        model pO2 = reactor time replicat(reactor) reactor*time /ss3;
        test h=reactor e=replicat(reactor);
run;
```

//sas program used to compare the curves in Figure 3.3a_b

```
options ls=78 nodate;
data one;
        infile 'c:\weicheng\12.prn';
        input reactor $ time replicat pO2_difference;
proc glm data=one;
        class reactor time replicat;
        model pO2_difference = reactor time replicat(reactor) reactor*time /ss3;
        test h=reactor e=replicat(reactor);
run;
```

//sas program used to compare the curves in Figure 3.3a_c

```
options ls=78 nodate;
data one;
        infile 'c:\weicheng\9.prn';
        input reactor $ time replicat pCO2;
proc glm data=one;
        class reactor time replicat;
        model pCO2 = reactor time replicat(reactor) reactor*time /ss3;
        test h=reactor e=replicat(reactor);
run;
```

//sas program used to compare the curves in Figure 3.3a_d

```
options ls=78 nodate;
data one;
        infile 'c:\weicheng\17-.prn';
        input reactor $ time replicat pCO2_difference;
proc glm data=one;
        class reactor time replicat;
        model pCO2_difference = reactor time replicat(reactor) reactor*time /ss3;
        test h=reactor e=replicat(reactor);
run;
```

//sas program used to compare the curves in Figure 3.3b

```
options ls=78 nodate;
data one;
        infile 'c:\weicheng\12.prn';
        input reactor $ time replicat pO2_difference;
proc glm data=one;
        class reactor time replicat;
        model pO2_difference = reactor time replicat(reactor) reactor*time /ss3;
        test h=reactor e=replicat(reactor);
run;
```

//sas program used to compare the curves in Figure 3.3c

```
options ls=78 nodate;
data one;
        infile 'c:\weicheng\17-.prn';
        input reactor $ time replicat pCO2_difference;
proc glm data=one;
        class reactor time replicat;
        model pCO2_difference = reactor time replicat(reactor) reactor*time /ss3;
        test h=reactor e=replicat(reactor);
run;
```

//sas program used to compare the curves in Figure 3.3d

```
options ls=78 nodate;
data one;
        infile 'c:\weicheng\17-.prn';
        input oxygen_level $ time replicat pCO2_difference;
proc glm data=one;
        class oxygen_level time replicat;
       model pCO2_difference = oxygen_level time replicat(oxygen_level)
oxygen_level*time /ss3;
        test h=oxygen_level e=replicat(oxygen_level);
run;
```

//sas program used to compare the curves in Figure 3.3e

```
options ls=78 nodate;
data one;
        infile 'c:\weicheng\20-.prn';
        input oxygen_level $ time replicat pO2_difference;
proc glm data=one;
        class oxygen_level time replicat;
        model pO2_difference = oxygen_level time replicat(oxygen_level)
oxygen_level*time /ss3;
        test h=oxygen_level e=replicat(oxygen_level);
run;
```

//sas program used to compare the curves in Figure 3.5

```
options ls=78 nodate;
data one;
        infile 'c:\weicheng\3.prn';
        input oxygen_level $ time replicat pH;
proc glm data=one;
        class oxygen_level time replicat;
        model pH = oxygen_level time replicat(oxygen_level) oxygen_level*time /ss3;
        test h=oxygen_level e=replicat(oxygen_level);
run;
```

//sas program used to compare the curves in Figure 3.6

```
options ls=78 nodate;
data one;
        infile 'c:\weicheng\6.prn';
        input oxygen_level $ time replicat glucose;
proc glm data=one;
        class oxygen_level time replicat;
        model glucose = oxygen_level time replicat(oxygen_level) oxygen_level*time
/ss3;
        test h=oxygen_level e=replicat(oxygen_level);
run;
```